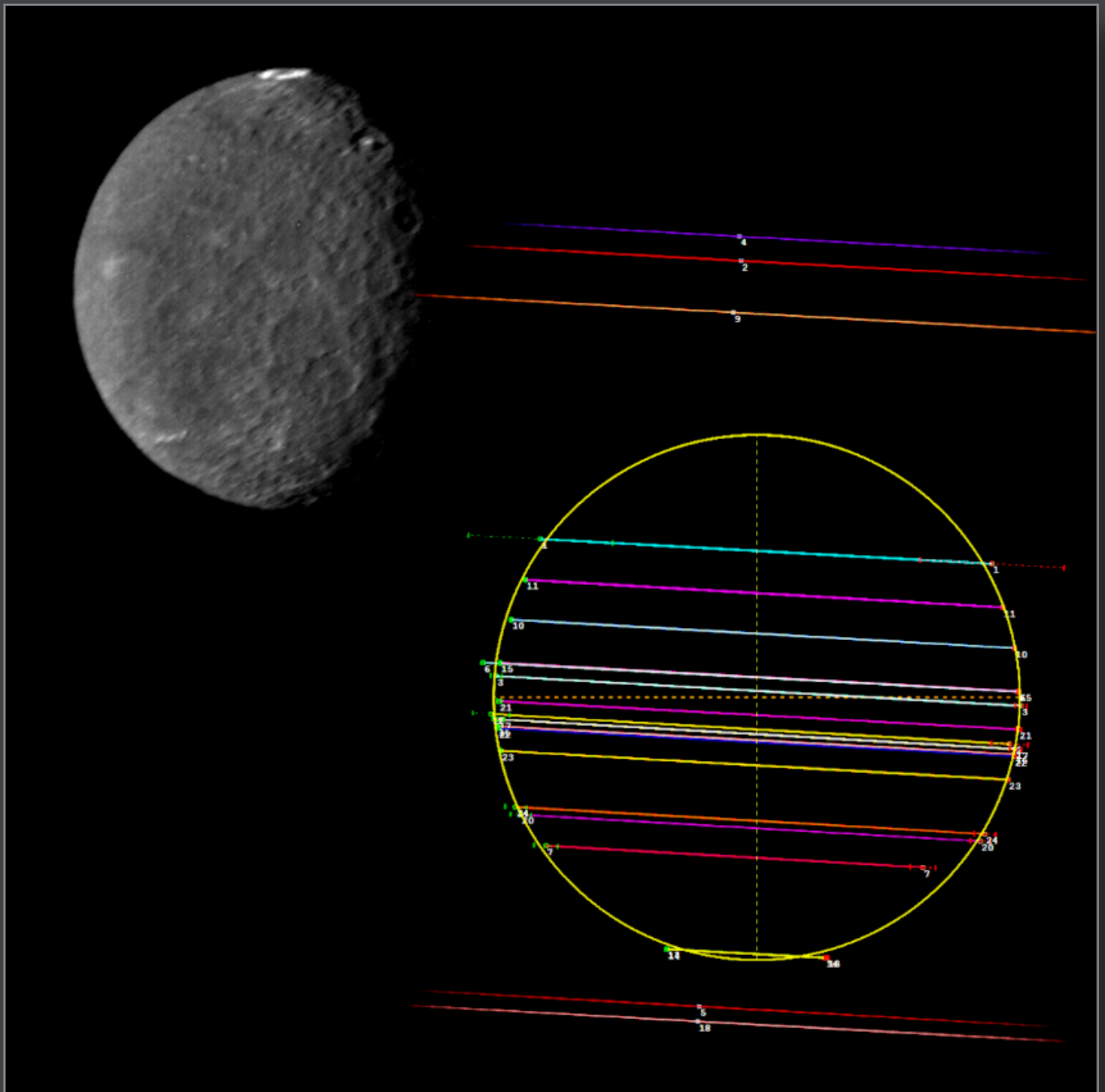


# *Journal for* **Occultation Astronomy**



Volume 11 · No. 1

2021-01



2020 Sep 21 • First Observation of an Occultation by Uranus' Moon Umbriel

# Dear reader,

10 years of our Journal, 38 issues filled with articles and reports about occultation work, all this was only possible with YOU, reading and writing articles about all aspects of occultation astronomy.

In these years we saw great scientific revolutions in occultation astronomy. The Gaia mission provides us with excellent star catalogues with an unprecedented precision. The imaging technology advanced from analogue video to digital. Software for photometric analyses has been developed to ease the use of digital cameras.

And our view of the solar system got widely expanded. Occultation astronomy found out, that tiny bodies can have rings only a few kilometres wide. The space mission to Pluto and further afield showed that we can provide tools for measuring faint atmospheres. And not only once in a lifetime as space missions can do. The combination of photometry and occultation work leads us to insights into the 3-dimensional shape of bodies in the solar system. But questions remain, such as: Why are there no main belt asteroids having rings? Is this by chance or some law behind it?

The next ten years... A broad discussion is needed, what IOTA should do in the future. Our ESOP and other international meetings as well as our JOA give us great platforms. I would like, that YOU, the reader of JOA takes part in this and communicate, what you suggest for future work. Just observing occultations for the decade to come is "more of the same". There are so many questions out there, in combination with professional and amateur work (PRO-AM) we should be able to contribute to answers.

With all the best to you

**Wolfgang Beisker**

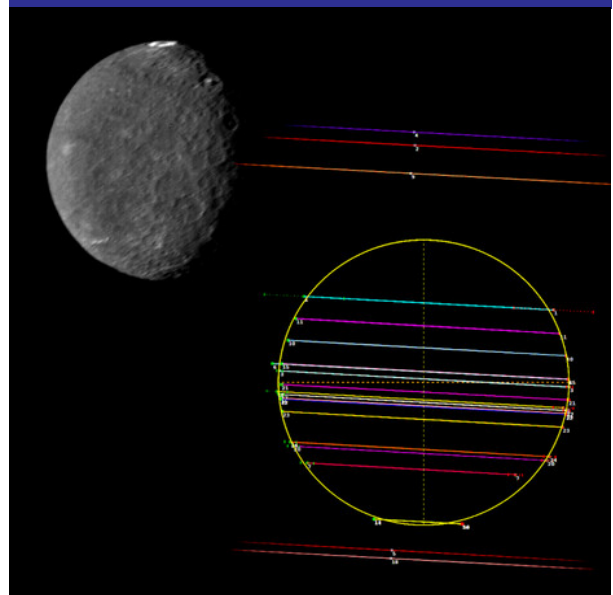
Wolfgang Beisker, IOTA/ES - Research & Development

JOA Volume 11 · No. 1 · 2021-1 \$ 5.00 · \$ 6.25 OTHER (ISSN 0737-6766)

## In this Issue:

■ <b>Participating in PHEMU21</b> Alex Pratt, Nikolai Wünsche. . . . .	3
■ <b>Grazing Occultations of Stars by the Moon in 2021</b> Eberhard Riedel. . . . .	10
■ <b>The Shelyak TimeBox - A Device Allowing Multi-Mode Accurate UTC Time Recordings for Digital Video Cameras</b> Cesar Valencia Gallardo, Dave Gault, Thierry Midavaine, Hristo Pavlov. . . . .	22
■ <b>Beyond Jupiter: (55576) Amycus</b> Konrad Guhl. . . . .	32
■ <b>The International Occultation Timing Association's 38<sup>th</sup> Annual Meeting, July 25-26 via Zoom Online</b> Richard Nugent . . . . .	36
■ <b>Breaking News</b> . . . . .	43
■ <b>Imprint</b> . . . . .	44

## COVER



An occultation by Umbriel was observed on 2020 Sep 21 for the first time. Observing stations in the US and Canada recorded 20 positive and 5 negative chords for a shape profile of this moon of Uranus. The observers measured Umbriel's diameter to be 1169 km from an observing distance of 19 AU. During the flyby in early 1986 the *Voyager 2* space probe captured the image of the darkest of the larger moons of Uranus from a distance of 557,000 km. Graphic: O. Klös, made with an image from NASA/JPL and data from *Occult*

## Copyright Transfer

Any author has to transfer the copyright to IOTA/ES. The copyright consists of all rights protected by the worldwide copyright laws, in all languages and forms of communication, including the right to furnish the article or the abstracts to abstracting and indexing services, and the right to republish the entire article. IOTA/ES gives to the author the non-exclusive right of re-publication, but appropriate credit must be given to JOA. This right allows you to post the published pdf Version of your article on your personal and/or institutional websites, also on ArXiv. Authors can reproduce parts of the article wherever they want, but they have to ask for permission from the JOA Editor in Chief. If the request for permission to do so is granted, the sentence "Reproduced with permission from *Journal for Occultation Astronomy*, JOA, ©IOTA/ES" must be included.

## Rules for Authors

In order to optimize the publishing process, certain rules for authors have been set up how to write an article for JOA. They can be found in "How to Write an Article for JOA" published in this JOA issue (2018-3) on page 13. They also can be found on our webpage at [http://www.iota-es.de/how2write\\_joa.html](http://www.iota-es.de/how2write_joa.html) .

# Participating in PHEMU21

Alex Pratt · IOTA/ES · BAA · Leeds · England · alex.pratt@bcs.org.uk  
Nikolai Wünsche · IOTA/ES · Biesenthal · Germany · nwuensche@astw.de

**ABSTRACT:** Every 6 years the orbital plane of Jupiter’s Galilean satellites is edge-on to the Earth and these moons undergo a series of mutual eclipse and occultation phenomena, known as PHEMUs. This next occurs in 2021 and this article describes how to take part in the PHEMU21 campaign: to obtain accurately timed photometry of these events to contribute to studies of the satellites’ orbits.

## Introduction

In his PHEMU 2021 presentation to ESOP XXXIX [1], Josselin Desmars (IMCCE)<sup>1</sup>, explained that mutual satellite events, PHEMUs<sup>2</sup>, occur when the Earth crosses the orbital plane of a planet’s satellites (for occultations) and/or when the Sun crosses this plane (for eclipses). Photometry of the Jovian events in 2021 can produce high-quality astrometry of its Galilean moons<sup>3</sup>.

In their paper in *JOA 2020-4*, Jean-Eudes Arlot (IMCCE, Paris) and Nicolai Emelyanov (Sternberg Astronomical Institute, Moscow State University) promoted PHEMU21 [2], the pro-am campaign to observe the mutual occultations and eclipses of the Galilean satellites of Jupiter in 2021. They described the PHEMU events in

detail, the history of observing campaigns and why they are of value to professional astronomers and spaceflight engineers. They explained how to obtain good quality photometry, how the data are reduced, and how to obtain predictions and submit observations. This article complements their work, giving advice to amateurs taking part in PHEMU21.

## The Circumstances in 2021

The PHEMU events occur between 2021 January 3 and November 16, although Jupiter is at conjunction with the Sun on January 29, so after early January observations cannot resume until March, reducing the observing window. Jupiter reaches opposition on the night of Aug 19 when its declination will be -14 degrees (Figure 1), so unlike PHEMU15 (2014-2015), this apparition favours observers in the southern hemisphere.

<sup>1</sup> Institut de mécanique céleste et de calcul des éphémérides · Observatoire de Paris

<sup>2</sup> Phénomène mutuel (French) – Mutual phenomena (English)

<sup>3</sup> Eclipses of Amalthea and Thebe will also occur, but they are very faint.

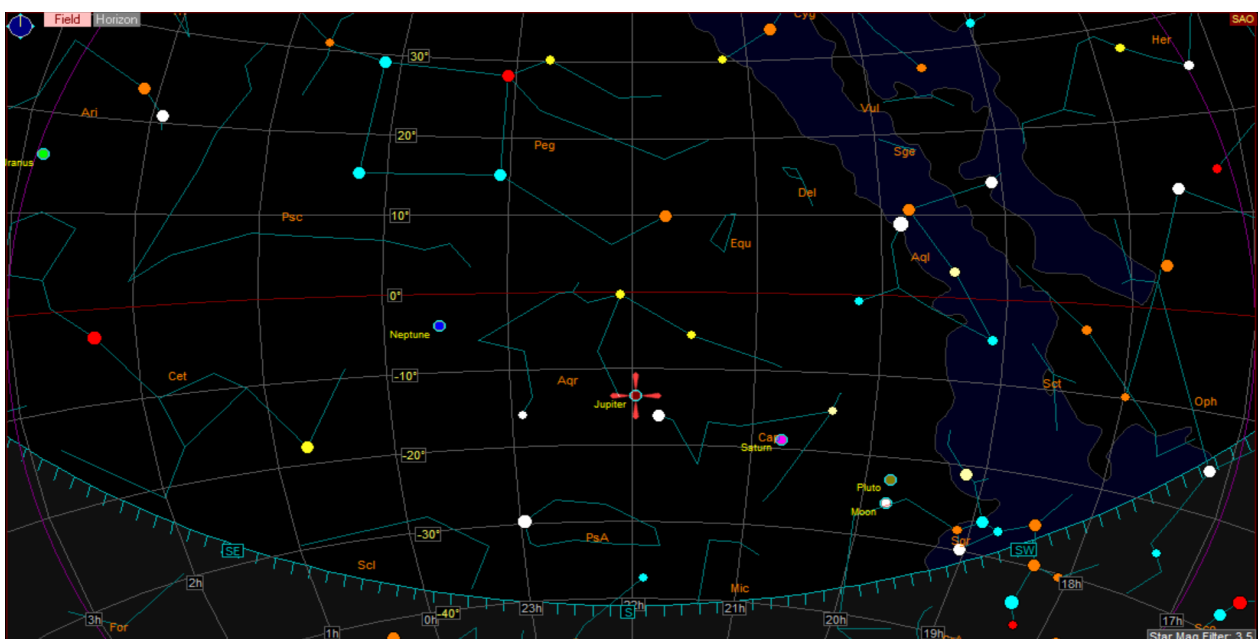


Figure 1. Jupiter at opposition on 2021 August 19-20, as seen from Paris (Graphic: C2A)

## Predictions

IMCCE-SAI have provided a webpage for observers to list all events that will occur from their location (Figure 2), [3].

By default, the observatory code is 500 (geocentric location), and clicking on the 'Show' button will list a full set of events. Clicking on 'the list' link displays all observatory codes. If you have an

MPC code use that, otherwise entering the code of an observatory in your country or your region of the world will suffice. This field is case sensitive, so you must use uppercase letters. It will list all events visible from your chosen observatory, including daytime events.

Selecting observatory code 007 (Observatoire de Paris, France) lists a total of 28 events (Figure 3).

Figure 2. The IMCCE PHEMU21 predictions webpage.

```
v5.20.11i Planet: Jupiter CALCEPH: (INPOP17a)
Planet
Observatory N: 007 - Paris
Timescale: UTC
Mean equator and equinox of J2000. ICRF.

Mutual events of satellites:
Date begin: h m s end: h m s Type Dur(m) Impact m Δm limb(") dist(") Planet(°) Sun(°) Moon phase
2021 1 7 15 9 23 15 43 47 201 34.4 0.369 5.1 0.328 70.18 : 16.534 7.269 0.410
2021 1 7 16 42 14 17 6 13 2E1 24.0 0.057 5.1 0.870 77.00 6.12 : 6.717 -4.879 0.406
2021 1 18 8 54 39 9 6 42 201 12.0 0.431 5.1 0.279 79.10 : 6.302 9.305 0.350
2021 2 28 7 0 9 7 11 10 4E2 11.0 0.212 5.4 0.947 80.99 40.26 : 9.513 3.395 0.920
2021 3 14 6 34 28 6 39 34 103 5.1 0.903 4.7 0.016 81.35 : 12.457 3.949 0.064
2021 3 16 6 11 8 6 12 25 201 1.3 0.970 5.1 0.003 65.36 : 10.388 0.802 0.181
2021 3 18 5 7 11 5 12 53 401 5.7 0.129 5.2 1.113 13.21 : 2.417 -9.051 0.298
2021 3 26 4 50 4 4 57 19 1E4 7.3 0.481 5.2 0.295 34.08 73.37 : 3.977 -9.020 0.810
2021 3 28 4 37 14 4 40 29 102 3.2 0.603 5.0 0.169 35.53 : 3.111 -10.366 0.952
2021 4 4 5 26 21 5 31 2 1E2 4.7 0.396 5.0 0.506 57.38 36.29 : 13.304 -0.029 0.510
2021 4 12 4 16 38 4 42 54 1E4 26.3 0.098 5.1 0.483 8.43 63.36 : 7.793 -8.423 0.023
2021 4 17 3 9 17 3 13 26 2E1 4.1 0.692 4.9 0.170 69.39 38.58 : 0.430 -16.338 0.307
2021 4 24 5 24 12 5 27 30 2E1 3.3 0.805 4.9 0.085 68.11 42.55 : 21.354 5.853 0.779
2021 4 27 2 34 7 2 40 46 2E3 6.7 0.696 4.6 0.162 51.73 69.46 : 0.512 -17.447 0.983
2021 5 6 3 26 34 3 32 5 1E2 5.5 0.159 4.8 0.626 86.55 46.06 : 12.887 -8.533 0.342
2021 5 14 3 43 53 3 52 43 3E1 8.8 0.162 4.4 0.567 56.22 67.49 : 18.742 -4.425 0.147
2021 5 21 2 36 9 2 40 23 3E2 4.2 0.905 4.4 0.036 97.09 76.13 : 13.612 -11.408 0.596
2021 5 29 2 27 55 3 17 31 3E1 49.6 0.145 4.3 0.567 36.61 42.13 : 16.448 -11.052 0.790
2021 6 7 1 36 22 1 41 18 1E2 4.9 0.648 4.6 0.205 112.72 45.15 : 14.238 -16.614 0.200
2021 6 14 3 53 58 3 58 33 1E2 4.6 0.736 4.5 0.130 117.69 43.07 : 28.990 0.240 0.237
2021 7 4 0 6 19 0 10 0 3E1 3.7 0.896 4.0 0.040 85.08 64.74 : 16.193 -18.402 0.365
2021 7 7 0 47 13 0 49 3 1E3 1.8 0.970 4.0 0.005 96.70 65.92 : 22.174 -17.763 0.184
2021 7 9 0 5 54 0 7 19 1E2 1.4 0.985 4.4 0.002 130.49 30.49 : 18.543 -18.924 0.064
2021 8 1 22 0 49 0 5 35 302 124.8 0.997 4.0 0.000 149.17 : 15.055 -18.744 0.415
2021 8 8 20 13 42 21 18 44 3E2 65.0 0.635 4.0 0.205 84.22 7.68 : 4.181 -8.856 0.034
2021 8 9 3 37 8 4 44 41 3E2 67.5 0.343 4.0 0.465 174.12 6.66 : 17.412 -9.010 0.050
2021 8 19 4 15 7 4 34 14 1E3 19.1 0.709 3.9 0.112 3.19 2.92 : 6.158 -6.013 0.760
2021 8 30 19 2 52 19 15 28 3E2 12.6 0.766 4.0 0.120 205.20 13.26 : 7.250 -5.013 0.470
```

Figure 3. IMCCE PHEMU21 predictions for Paris Observatory.

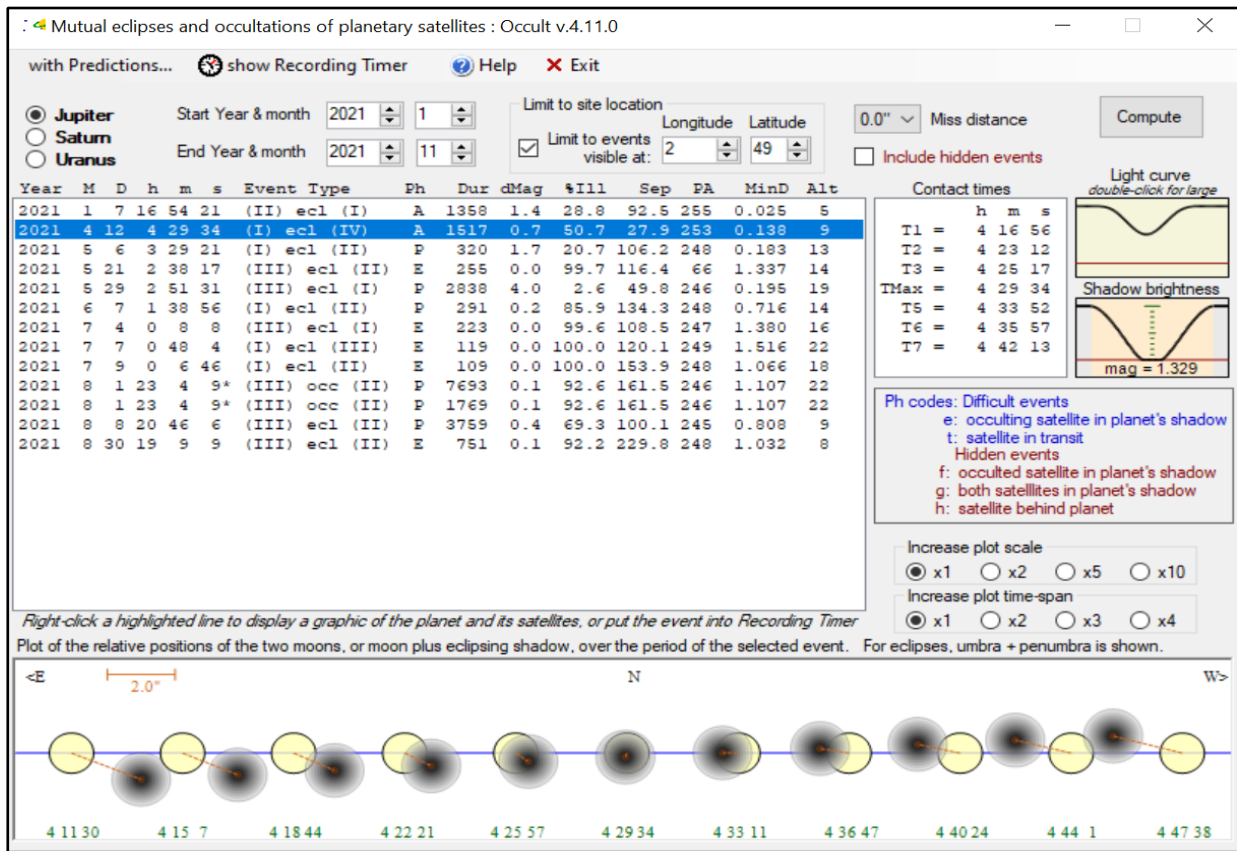


Figure 4. Occult PHEMU21 predictions for Paris Observatory.

Dave Herald's *Occult* [4] can also be used to compute predictions for any location. From its main menu, select 'Satellite phenomena' – 'Mutual eclipses & occultations'. This opens a predictions page. To compute predictions at a specific location, e.g. Paris: Set 'Start Year & month' to 2021 01, and 'End Year & month' to 2021 11. Set 'Longitude' to 2 (East is positive), and 'Latitude' to 49. Tick the box 'Limit events visible at:', then click 'Compute'. This will list the events when the Sun is at least 6 degrees below the horizon and Jupiter has an altitude greater than 5 degrees at the mid-time of the PHEMU (Figure 4).

It lists 13 PHEMUs observable from Paris. Column 'dMag' gives the predicted drop in combined magnitude during an eclipse. The entries for August 1 are marked with an asterisk, indicating they are slow, long-duration events of close-moving satellites and the iterative solution has not converged. Arbitrarily selecting favourable entries with 'dMag' of at least 0.2 gives only 6 good targets from Paris (Table 1).

After highlighting an event in the *Occult* predictions page, it displays contact times and a light curve on the right-hand side, and a timeline at the bottom of the page. Double-clicking on an entry opens a diagram of Jupiter with the positions of the respective satellites (Figure 5). This is most useful for correctly identifying the target and reference moons.

Dave Herald further developed these features during PHEMU15 and the predictions and diagrams are available in the Planet Satellites feed to *Occult Watcher*, maintained by Hristo Pavlov. This is available during PHEMU21. In some cases, observers were caught out by a minimum that was deeper than expected; hopefully this will not occur in this campaign.

Location	Events
Athens, GR	9
Dehli, IN	15
Dunedin, NZ	26
Los Angeles, US	11
Paris, FR	6
Pulkovo, RU	1
Rio de Janeiro, BR	13
Rome, IT	5
Sydney, AU	24
Tokyo, JP	16
Tunis, TN	10
Washington, D.C.	12

Table 1. Probable numbers of PHEMUs at selected locations – arbitrary dMag limit of 0.2.

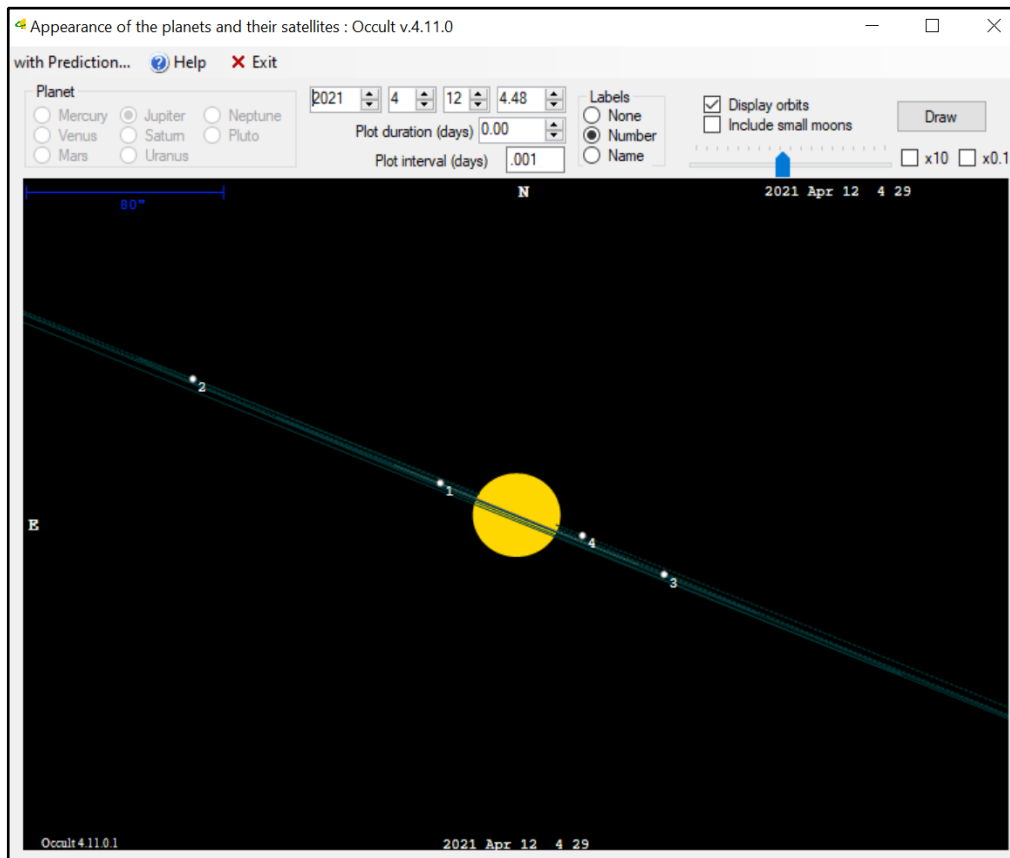


Figure 5. Occult PHEMU21 schematic of the event on 2021 April 12.

## Telescope, Camera and Mount

The Galilean satellites are bright and at opposition their magnitudes range from 4.4 to 5.5, so a small telescope can be used to observe them. During PHEMU15 good quality photometry was obtained with telescope apertures as small as 7 cm [5], [6]. Use a focal length that includes at least one reference moon in the field. The light of each moon should be distributed over several pixels. For short focal lengths, slightly defocus the moons. Most observers submit unfiltered observations; a red filter could be used to darken the sky background or a methane filter to reduce the glare from Jupiter [1].

In 2014-2015, the authors used the following optical equipment:

- 20 cm SCT at 200 cm, 132 cm and 66 cm focal lengths
- 28 cm SCT at 92 cm focal length
- 15 cm reflector at 225 cm, 128 cm and 120 cm focal lengths

The shorter focal lengths were achieved using focal reducers.

They employed the following cameras:

- Wattec 910HX analogue video camera
- QHY5L-II mono CMOS digital camera

The Wattec analogue camera is 8-bit technology, but a digital camera, such as the 12-bit QHY174M-GPS, has a bigger well depth and a wider dynamic range, and can give more accurate photometry, producing smoother, better-quality light curves; use the camera's highest quality output setting.

The telescope mount will be tracking on events for several minutes, so make sure it is accurately polar aligned, has minimal backlash in the RA axis, and there is no 'jitter' in the drive.

## Recording

The observer has a wide choice of recording software, such as *FireCapture* [7], *IOTA\_VideoCapture* [8], *Limovie* [9], *OccuRec* [10], *SharpCap* [11] and *VirtualDub* [12]. These programs support a broad range of analogue and digital cameras, and offer AAV, AVI, FITS and SER output formats. Most of these file systems will create large files over the duration of a PHEMU, up to several gigabytes in size, so your computer must have sufficient storage space.

*OccuRec* is recommended for integrating analogue video cameras – it detects the camera's integration setting, averages all repeated frames during this interval, and outputs an AAV file which is usually much smaller than an AVI or SER file over the same recording period. Hristo Pavlov (*OccuRec* developer) recommends the following settings for recording PHEMUs:

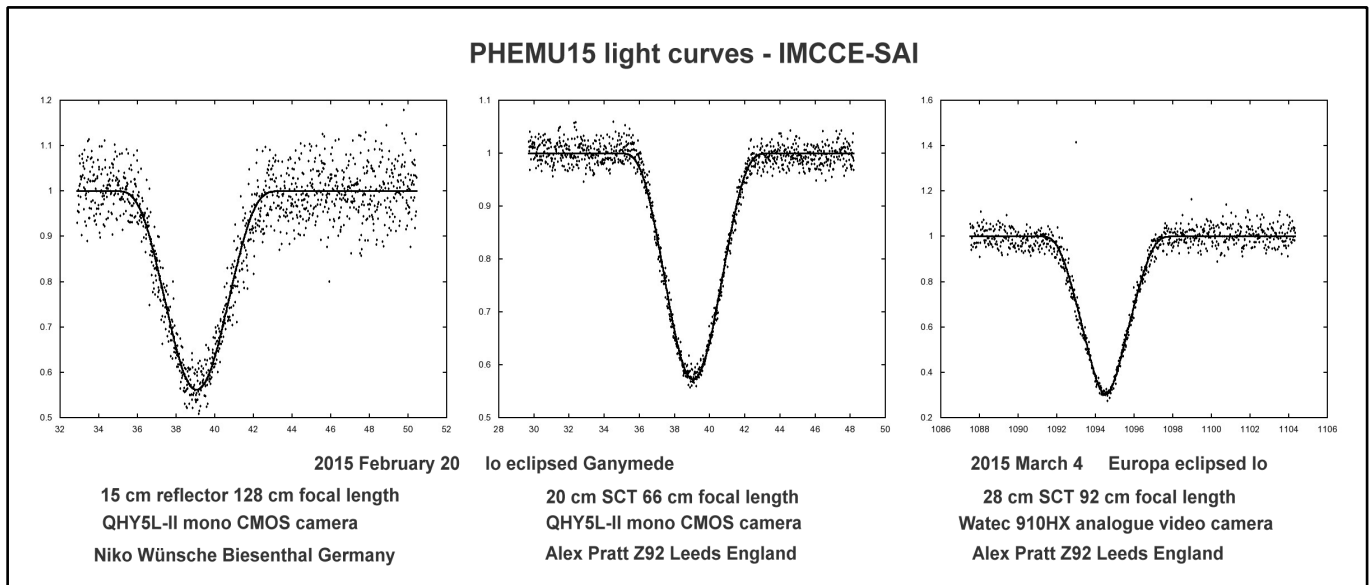


Figure 6. Examples of PHEMU15 light curves recorded with QHY5L-II and Watec 910HX cameras [13].

- From the Settings, go to “Advanced” tab, tick “ADV Compression” and choose “Lagarith 16”
- From the Settings, go to “Astro Analogue Video (AAV)” and for “Pixel Integration” ensure that “Binning (16 bit, x256 Max Integration)” is selected
- Once you have the system running, use the following integration settings:
- Set your integrating camera to no integration or to use exposures shorter than 1 video frame. Non-integrating video camera can be also used.
- Set a ‘Manual’ integration of x1 and ‘Lock’ the integration rate.
- Click the “x1 Stacking” button and choose a stacking mode. Adjust the stacking timespan according to the expected event duration and wind conditions. For example, for a 2-hour event you can use x128 or x64 stacking while for 5 min event you should use x2 or x4 stacking. If you have windy conditions, consider using smaller stacking in order to avoid trailed images.

Programs such as *FireCapture* and *SharpCap* are recommended for digital cameras. They allow full control over the exposure time, gain, binning and region of interest, etc. Authors ARP and NW used *FireCapture* with their QHY5L-II CMOS cameras during PHEMU15.

The Galilean moons are bright, so do not use a high gain setting and avoid image saturation. A good signal-to-noise ratio is required and most recording software has a feature to display the point spread function gaussian curve of a target, to assist in choosing the exposure time / integration interval. Roger Venable (IOTA) has analysed the response of the popular Watec 910HX camera and discussed its non-linearity [14], so be aware of how this could affect your recording.

In 2014-2015 the authors used integration settings of 0.16 s and 0.32 s with analogue cameras, and exposures of 0.2 s to 0.25 s with digital cameras. Do a test recording before each PHEMU

event. Later in the campaign ARP also took dark and flat field recordings for calibrating the PHEMU videos. *Tangra* [15] supports bias and dark frame and flat field FITS images, either saved by digital cameras or created from short videos. (See *Appendix*). Observers should record the target field for 5 minutes before and after the start and end times of an event [1]. This is to assist the photometric reduction and analysis by measuring the flux level outside the PHEMU event window.

### Timing

IMCCE-SAI require photometric estimates with a timing accuracy of 0.1s. Occultation observers are accustomed to this requirement, but if you do not know the accuracy of your equipment you should check it before recording any PHEMUs [16],[17].

In 2014-2015, ARP used a 1PPS IOTA-VTI to provide an accurate time-base for the Watec 910HX analogue camera. When recording with the QHY digital camera, *Dimension 4* [18] was used to set the laptop’s clock. Unlike a full implementation of NTP (Network Time Protocol), which applies small time increments / decrements to slowly drift the computer clock into synchronisation, *Dimension 4* uses SNTP (Simple NTP) and it ‘kicks’ the computer clock, so it can produce sudden jumps >1 s in the time-of-day. For this reason, ARP disabled *Dimension 4* immediately before each PHEMU event and reactivated it afterwards. NW used *Meinberg NTP* [19], [20] to maintain accurate and stable time on his laptop computer; a fast internet connection is required [17].

During 2014-2015 ARP used 2 versions of *FireCapture*. Tests against the 1PPS LED of the IOTA-VTI indicated that one version of the software wrote its timestamps at the start of each exposure; the other version wrote them at the end of each exposure. Appropriate corrections were applied to the data sent to the IMCCE-SAI.

## Analysing the Video

These notes apply to users of *Tangra*.

- Open the PHEMU video. (If applicable, load the dark and flat FITS files. See *Appendix*)
- Click Reduction – Light Curve Reduction (Photometry) – Tracked Mutual Satellite Event – select Occultation or Eclipse
- Select and Add Object. *Tangra* will open a Mutual Event target box. Select the occulted or eclipsed ‘star(s)’ and repeat the process for the reference ‘star(s)’. Analyse the video.
- You can normalise the light curve for presentation purposes, but this is not necessary when submitting data to IMCCE-SAI. By default, *Tangra* applies Average Background. The Data tab offers a range of processing options, where Quick Re-Process is useful to review the effects, e.g. Median Background is useful in the case of ‘light spill’ from another satellite or from Jupiter. In general, Aperture Photometry is recommended for bright, large or defocused moons; PSF Photometry is better when they are small, in focus and not heavily saturated.
- Exporting the CSV file  
File – Export Light Curve – Save as CSV File – Timestamps offers 3 options: HH:m:ss.fff, Days with decimals, or Julian Day with decimals. The latter option is the most straightforward when submitting the data section of the CSV to IMCCE-SAI.

## Submitting Observations

IMCCE-SAI have published a webpage for observers to submit their observations (Figure 7), [21].

The first step is to obtain a unique operator ID then carefully read the information in the ‘see explanation’ links.

In 2015 some observers found the process complicated and confusing, so they didn’t submit their data. The contact addresses of IMCCE and SAI are given in the ‘Credit’ link of the above website and in the *JOA* paper [2] and they are most helpful. Observers on your regional Occultations forum should also be able to assist.

## Concluding Remarks

PHEMU21 offers fewer mutual eclipses and occultations than in the previous campaign, particularly for locations in the northern hemisphere. This makes it more important that we try to record some events and submit quality data to the IMCCE-SAI.

## Acknowledgements

The authors wish to thank Hristo Pavlov and Dave Herald for their help and advice with *OccuRec*, *Tangra* and *Occult* and the IMCCE and SAI staff during the PHEMU15 campaign.

Not secure | www.sai.msu.ru/neb/nss/phemuobsai.htm

---

**Natural Satellites Service.** Uploading observation of mutual events (v.20.11.20)

---

**This is a tool for automatic input** of the photometric observations of the mutual occultations and eclipses of the galilean satellites of Jupiter in 2021 in the database.

---

**To start** entering your data, send email to **phemu@imcce.fr** to obtain a unique operator ID.

---

**To see** your previously entered data  
Input your operator ID  and  
Event observation ID   
(Leave this field blank to get the list of your entered observations)

Select:  show first and last lines only    show all the data  
Then press

---

**To input** your results of observation for **one mutual phenomenon** enter or choose the following information and press **Submit** (below).  
You will **receive** on a separate page an unique identification code for this observation (**Event observation ID**) followed by your data.  
**Remember** this **Event observation ID** for subsequent operations.

Input your operator ID

**Event identification** ( [See explanation](#) )

- Event beginning time:  
year  month  day  hour  minute
- Event:
- Type of the photometric measurement:  
 **occultation**    **eclipsed satellite only**    **eclipsed and eclipsing together**

Figure 7. IMCCE PHEMU21 website for submitting observations.

## Appendix

### Dark frame and flat field calibration of video recordings

CCD photometrists routinely apply dark frame and flat field corrections to their images. These techniques are not mandatory for PHEMU21, but if applied correctly to the videos they should improve the quality of photometric data submitted to the IMCCE-SAI. *Tangra* supports FITS dark frames and flat fields, either saved from a digital camera or created from an analogue video recording. (Remember to disable the timestamp display or disconnect the VTI feed).

### To make a dark frame video:

Cover the aperture of the telescope. Without the embedded timestamps, *OccuRec* will have difficulty detecting the integration setting of the dark field, so Hristo Pavlov recommends:

- Manually enter an integration rate of x1.
- Set a stacking rate that matches your camera integration rate/exposure.

Using the *same exposure and gain as the PHEMU video*, save a 20s video and include 'PHEMU dark' in its filename. This will be the 'Dark (Same Exposure)' video for use in *Tangra* calibration.

### To make a flat field video:

After selecting a uniform light source, e.g. white card, twilight sky, etc., adjust the exposure and gain settings so that the background intensity is roughly half of the full well depth (i.e. it should not be too dark and not too bright) and save the 20s video as 'flat'. Also, take a dark frame video for the flat field with the *same exposure and gain as the flat* and save it as 'dark for flat'.

*Tangra* can be used to create dark and flat FITS files from these videos:

- Create the Dark FITS
- Open the 'PHEMU dark' video.
- Click 'Reduction', 'Produce Bias, Dark or Flat Calibration Frame', 'Dark', enter the 'Effective Exposure' then click 'Produce Averaged Frame'. This creates a 'PHEMU dark'.fit file.
- Create the 'Dark for Flat' FITS
- Open the 'dark for flat' video and follow the above steps to create a 'dark for flat'.fit file.
- Create the Master Flat
- Open the 'flat' video.
- Click 'Reduction', 'Load Calibration Frame', 'Dark (Same Exposure)' but select the 'dark for flat'.fit. *Tangra* will indicate DARK at the bottom of the window.
- Click 'Reduction', 'Produce Bias, Dark or Flat Calibration Frame', 'Master Flat', 'Produce Average Frame' and save as 'master flat'.fit.
- To apply these calibrations to a PHEMU recording in *Tangra*, open the PHEMU video, click 'Load Calibration Frame', 'Dark (Same Exposure)' and select the 'PHEMU dark' fit file. Repeat this and

load the 'master flat'.fit. *Tangra* will indicate DARK and FLAT at the bottom of the window.

## References

- [1] Desmars, J., et al. PHEMU21: Mutual Phenomena of Jupiter Satellites in 2021 [https://esop39.iota-es.de/lections/esop\\_desmars.pdf](https://esop39.iota-es.de/lections/esop_desmars.pdf)
- [2] Arlot, J-E., Emelyanov, N. The Campaign of Observation of the Mutual Occultations and Eclipses of the Galilean Satellites of Jupiter in 2021. JOA 2020-04 pp. 3-10 [https://www.iota-es.de/JOA/JOA2020\\_4.pdf](https://www.iota-es.de/JOA/JOA2020_4.pdf)
- [3] <http://nsdb.imcce.fr/multisat/nsszph517he.htm>
- [4] Herald, D. Occult <http://www.lunar-occultations.com/iota/occult4.htm>
- [5] Saquet E. et al., The PHEMU15 catalogue and astrometric results of the Jupiter's Galilean satellite mutual occultation and eclipse observations made in 2014-2015, Monthly Notices of the Royal Astronomical Society, V 474, Issue 4, 4730-4739 (2018)
- [6] Natural Satellites Data Center – Mutual Events of the Galileans <http://nsdb.imcce.fr/obsphe/obsphe-en/fjuphemu.html>
- [7] Edelman, T. FireCapture <http://www.firecapture.de/>
- [8] IOTA\_VideoCapture <https://occultations.org/observing/software/>
- [9] Miyashita, K. Limovie [http://www.astro-limovie.info/limovie/limovie\\_en.html](http://www.astro-limovie.info/limovie/limovie_en.html)
- [10] Pavlov, H. OccuRec <http://www.hristopavlov.net/OccuRec/OccuRec.html>
- [11] Glover R. SharpCap <https://www.sharpcap.co.uk/>
- [12] Lee, A. VirtualDub <http://virtualdub.org/>
- [13] Pratt, A., Results from Participating in PHEMU15. ESOP XXXVII, Rokycany, Czechia. [http://www.esop37.cz/sbor/L5-1\\_Pratt\\_lecture.pdf](http://www.esop37.cz/sbor/L5-1_Pratt_lecture.pdf)
- [14] Venable, R. Some Idiosyncrasies of the Wattec 910HX Camera (PDF and YouTube video) 2020 Annual Meeting of IOTA <http://occultations.org/community/meetingsconferences/na/2020-iotaannual-meeting/presentations-at-the-2020-annualmeeting/>
- [15] Pavlov, H. *Tangra* <http://www.hristopavlov.net/Tangra/Tangra.html>
- [16] Gault, D., Herald, D. All-Of-System Time Testing Using Lunar Occultations. JOA 2020-01 pp. 9-13 [https://iota-es.de/JOA/JOA2020\\_1.pdf](https://iota-es.de/JOA/JOA2020_1.pdf)
- [17] Pavlov, H., Gault, D. Using the Windows Clock with Network Time Protocol (NTP) for Occultation Timing. JOA 2020-02 pp. 10-19 [https://www.iota-es.de/JOA/JOA2020\\_2.pdf](https://www.iota-es.de/JOA/JOA2020_2.pdf)
- [18] Dimension 4 <http://thinkman.com/dimension4/>
- [19] Wünsche, N. Precise computer clock setting with MS Windows. ESOP XXXVII, Rokycany, Czechia. [www.esop37.cz/sbor/L6-1\\_Wuensche\\_lecture.pdf](http://www.esop37.cz/sbor/L6-1_Wuensche_lecture.pdf)
- [20] Meinberg NTP for Windows [https://www.meinbergglobal.com/english/sw/ntp.htm#ntp\\_stable](https://www.meinbergglobal.com/english/sw/ntp.htm#ntp_stable)
- [21] <http://www.sai.msu.ru/neb/nss/phemuobsai.htm>

### Zoom Workshop on the PHEMU21 Campaign in French Language on 2021 Feb 06

Thierry Midavaine (Club Eclipse) has announced this workshop for the amateur community. Interested people should contact him to get the registration link. [thierrymidavaine@sfr.fr](mailto:thierrymidavaine@sfr.fr)

# Grazing Occultations of Stars by the Moon in 2021

Eberhard Riedel · IOTA/ES · München · Germany · e\_riedel@msn.com

**ABSTRACT:** The following maps and tables show this year's grazing occultations of the brightest stars and major planets by the Moon in those regions of the world where most of our observers live. The overall limiting magnitude is 5.0.

## Introduction

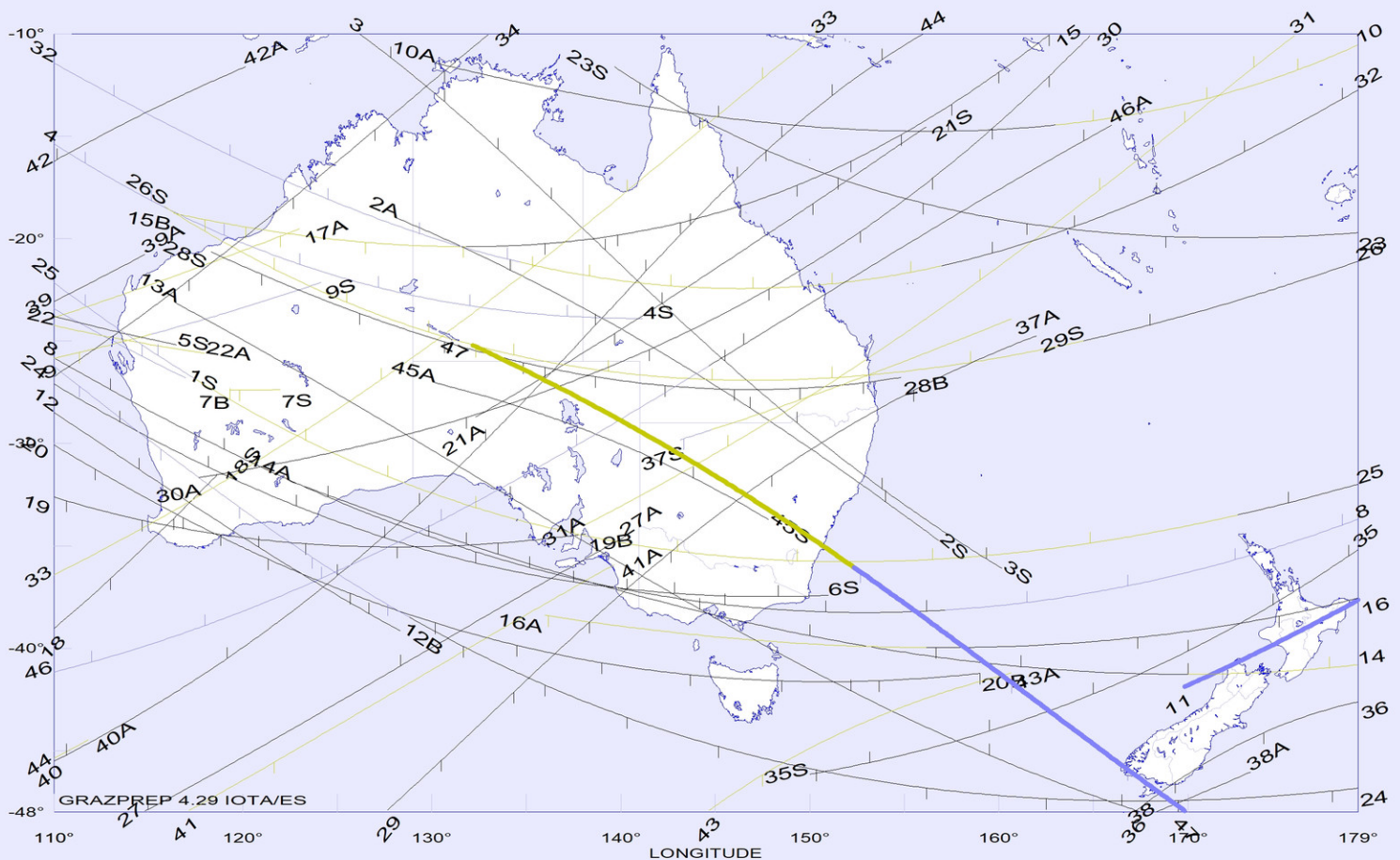
Nighttime events along the dark lunar limb are shown with a black line, whereas those events at night at the sunlit lunar limb are given in yellow. All daytime events appear in light blue. Events of stars or planets of 1.5 mag or brighter are highlighted with a bold line.

Tick marks appear along the limit lines every full 10 minutes of time. The northern limb grazes show tick marks pointing downwards, whereas on the southern limb grazes they point upwards.

All tables and pictures in this article were created with the author's

GRAZPREP-software. Further precise information on the local circumstances of all grazing occultations, also depending on the lunar terrain and the observer's elevation, is provided by this software which can be downloaded and installed via [www.grazprep.com](http://www.grazprep.com) (password: IOTA/ES) including prediction files that are needed additionally for different regions of the world. GRAZPREP assists in finding and listing individually favourable occultation events and in figuring out the best observing site in advance or even under way by graphically showing the expected apparent stellar path through the lunar limb terrain. The fainter stars are calculated with their highly precise positions from the Gaia-DR2-catalogue.

Grazing Occultations Australia-New Zealand 2021 <= 5.0 mag.

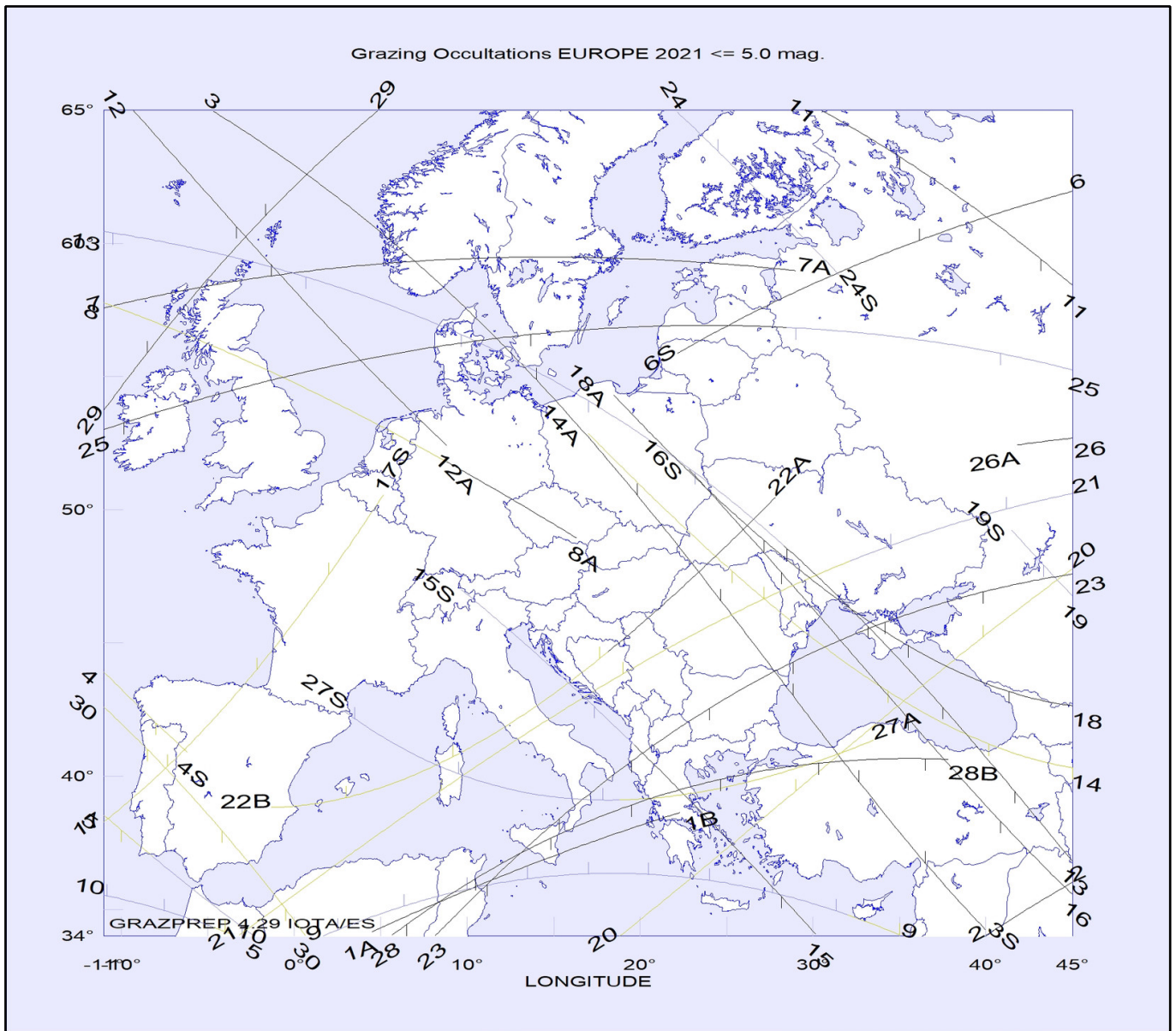


2021 Grazing Occultations Australia-New Zealand 2021 <= 5.0 mag. <small>GRAZPREP 4.27, IOTA/ES</small>												
No.	M D	USNO	SAOPPM D	MAG	%SNL	L.	W.UT	LONG	LAT	STAR NAME	MAG1	MAG2
1	Jan 02	ZC 1484	98955 C	3.5	84-	S	23 37.0	110	-23	eta Leonis NSV 04738	4.1	4.6
2	Jan 09	ZC 2322	159764 Y	4.1	15-	S	18 8.1	128	-19	Jabbah nu Scorpii	4.9	6.9
3	Feb 01	ZC 1773	119341 V	5.0	81-	S	17 5.0	126	-10	16 Virginis	5.8	5.8
4	Feb 05	ZC 2302	159682 H	2.6	36-	S	23 5.3	110	-15	Graffias beta 1 Scorpii	3.2	4.2
5	Mar 10	ZC 3175	164593	4.7	6-	S	22 11.6	110	-24	kappa Capricorni		
6	Apr 02	ZC 2513	185401 K	4.2	67-	S	18 52.6	110	-27	44 Ophiuchi NSV 08640	5.1	5.1
7	Apr 02	ZC 2523	185470	4.8	66-	N	21 59.0	119	-27	51 Ophiuchi NSV 09037		
8	Apr 03	ZC 2672	186841 w	2.8	56-	S	18 25.7	110	-26	Kaus Borealis lambda Sagittarii		
9	Apr 28	ZC 2302	159682 H	2.6	95-	N	22 38.6	110	-26	Graffias beta 1 Scorpii	3.2	4.2
10	May 05	ZC 3349	165321W	4.0	31-	S	17 15.8	130	-11	tau Aquarii NSV 14329		
11	May 12			-3.4	1+	N	20 49.7	170	-42	Venus		
12	May 27	ZC 2513	185401 K	4.2	98-	S	13 24.0	110	-28	44 Ophiuchi NSV 08640	5.1	5.1
13	May 28	ZC 2672	186841 w	2.8	94-	S	11 42.0	116	-23	Kaus Borealis lambda Sagittarii		
14	May 31	ZC 3164	164520 U	4.5	67-	S	14 18.2	122	-32	epsilon Capricorni	5.0	6.3
15	May 31	ZC 3175	164593	4.7	66-	N	16 55.3	116	-19	kappa Capricorni		
16	Jun 02	ZC 3428	146635 A	5.0	46-	N	15 20.6	136	-38	psi 3 Aquarii NSV 14491	5.2	11.2
17	Jun 22	ZC 2302	159682 H	2.6	94+	N	20 6.0	110	-24	Graffias beta 1 Scorpii	3.2	4.2
18	Jul 02	ZC 219	109926 w	4.8	39-	N	22 42.2	110	-39	mu Piscium		
19	Jul 20	ZC 2376	184450	4.5	84+	N	13 38.5	110	-33	omega Ophiuchi	4.5	4.5
20	Jul 21	ZC 2523	185470	4.8	91+	N	11 15.7	110	-30	51 Ophiuchi NSV 09037		
21	Aug 04	ZC 900	77775	4.8	13-	N	19 37.1	132	-29	139 Tauri		
22	Aug 11	ZC 1702	119035	4.0	10+	S	12 8.4	110	-24	nu Virginis		
23	Aug 14	ZC 2033	158427	4.2	36+	N	8 35.5	139	-12	kappa Virginis NSV 20060		
24	Aug 16	ZC 2302	159682 H	2.6	59+	N	7 57.2	110	-26	Graffias beta 1 Scorpii	3.2	4.2
25	Aug 16	ZC 2307	184123	3.9	60+	S	9 25.8	110	-22	Kow Kin omega 1 Scorpii		
26	Aug 16	ZC 2310	184135	4.3	60+	S	10 4.3	116	-18	Kow Kin omega 2 Scorpii		
27	Aug 18	ZC 2672	186841 w	2.8	83+	S	18 10.1	114	-48	Kaus Borealis lambda Sagittarii		
28	Aug 19	ZC 2809	187882 Q	4.9	89+	N	9 55.6	118	-21	psi Sagittarii	6.2	6.2
29	Aug 23	ZC 3419	146598 A	4.2	98-	N	18 32.8	127	-48	psi 1 Aquarii	4.5	8.5
30	Aug 26	ZC 219	109926 w	4.8	82-	N	13 53.4	117	-32	mu Piscium		
31	Aug 30	ZC 709	76721 L	4.3	46-	S	16 18.8	138	-34	tau Tauri	4.9	6.4
32	Sep 15	ZC 2750	187448 Y	2.0	68+	S	8 5.7	110	-11	Nunki sigma Sagittarii	2.9	2.9
33	Sep 26	ZC 656	76601 V	4.2	71-	S	16 13.1	110	-36	kappa Tauri NSV 01593	5.2	5.2
34	Sep 26	ZC 660	76608 V	4.3	71-	N	17 11.1	110	-27	upsilon Tauri	4.6	6.5
35	Oct 15	ZC 3164	164520 U	4.5	74+	S	8 25.5	150	-46	epsilon Capricorni	5.0	6.3
36	Oct 23	ZC 599	76430 S	4.4	92-	N	15 35.6	167	-48	37 Tauri		

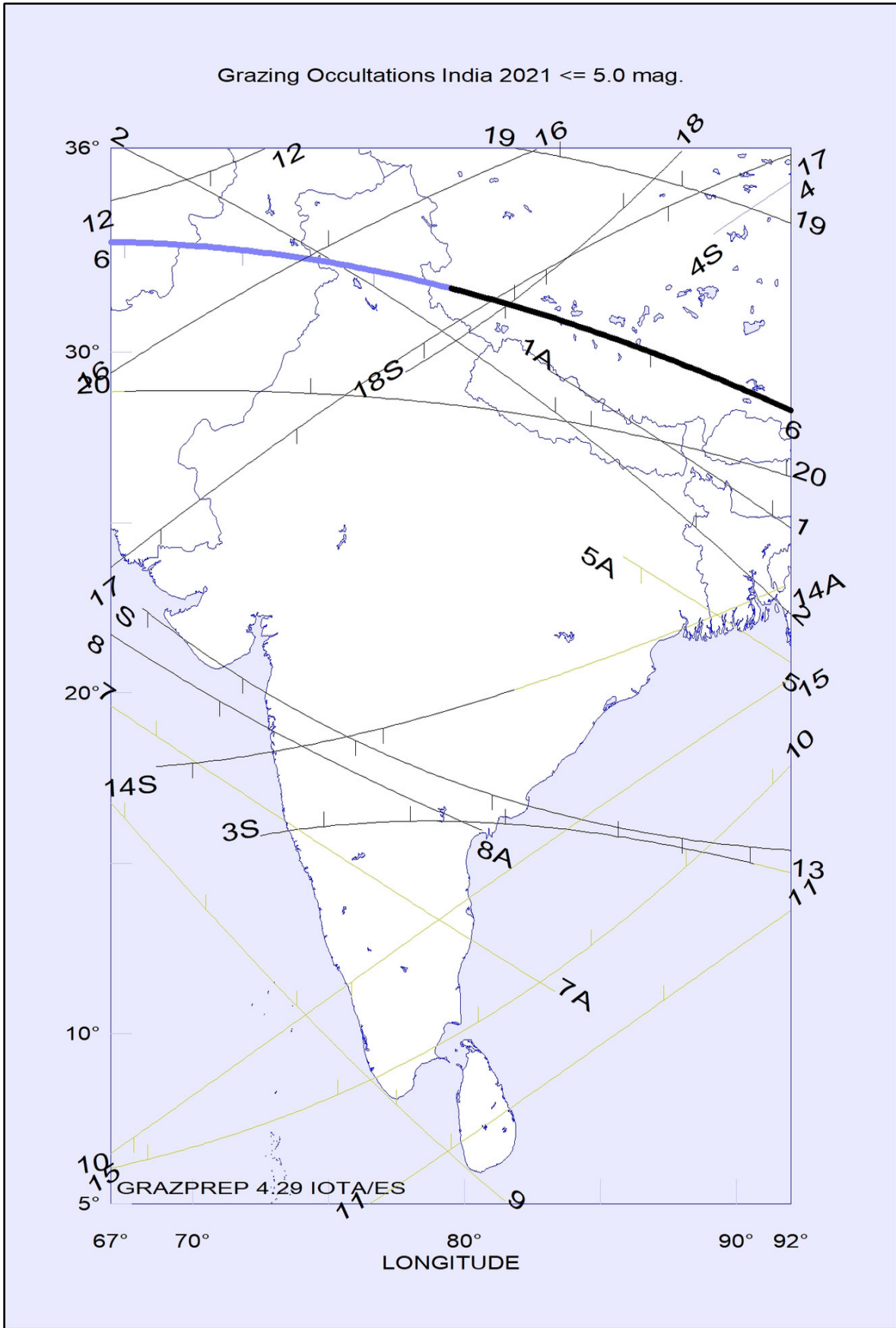
*(Continued on next page)*

# Australia & New Zealand

2021 Grazing Occultations Australia-New Zealand 2021 <= 5.0 mag. GRAZPREP 4.27, IOTA/ES												
No.	M D	USNO	SAOPPM D	MAG	%SNL	L.	W.UT	LONG	LAT	STAR NAME	MAG1	MAG2
37	Nov 06	ZC 2307	184123	3.9	3+	N	8 40.0	143	-30	Kow Kin omega 1 Scorpii		
38	Nov 06	ZC 2310	184135	4.3	3+	S	8 43.8	168	-48	Kow Kin omega 2 Scorpii		
39	Nov 07	ZC 2500	185320 J	3.3	10+	S	13 5.5	110	-23	theta Ophiuchi	3.6	5.6
40	Nov 07	ZC 2513	185401 K	4.2	10+	N	14 16.3	110	-45	44 Ophiuchi NSV 08640	5.1	5.1
41	Nov 08	ZC 2672	186841 w	2.8	19+	N	12 56.4	117	-48	Kaus Borealis lambda Sagittarii		
42	Nov 11	ZC 3164	164520 U	4.5	52+	S	16 10.5	110	-16	epsilon Capricorni	5.0	6.3
43	Nov 13	ZC 3419	146598 A	4.2	72+	N	15 6.6	144	-48	psi 1 Aquarii	4.5	8.5
44	Nov 16	ZC 219	109926 w	4.8	93+	S	11 59.5	110	-46	mu Piscium		
45	Dec 01	ZC 2033	158427	4.2	9-	S	18 42.2	130	-27	kappa Virginis NSV 20060		
46	Dec 06	ZC 2750	187448 Y	2.0	6+	S	8 6.9	110	-41	Nunki sigma Sagittarii	2.9	2.9
47	Dec 31			1.5	6-	N	18 30.9	132	-25	Mars		

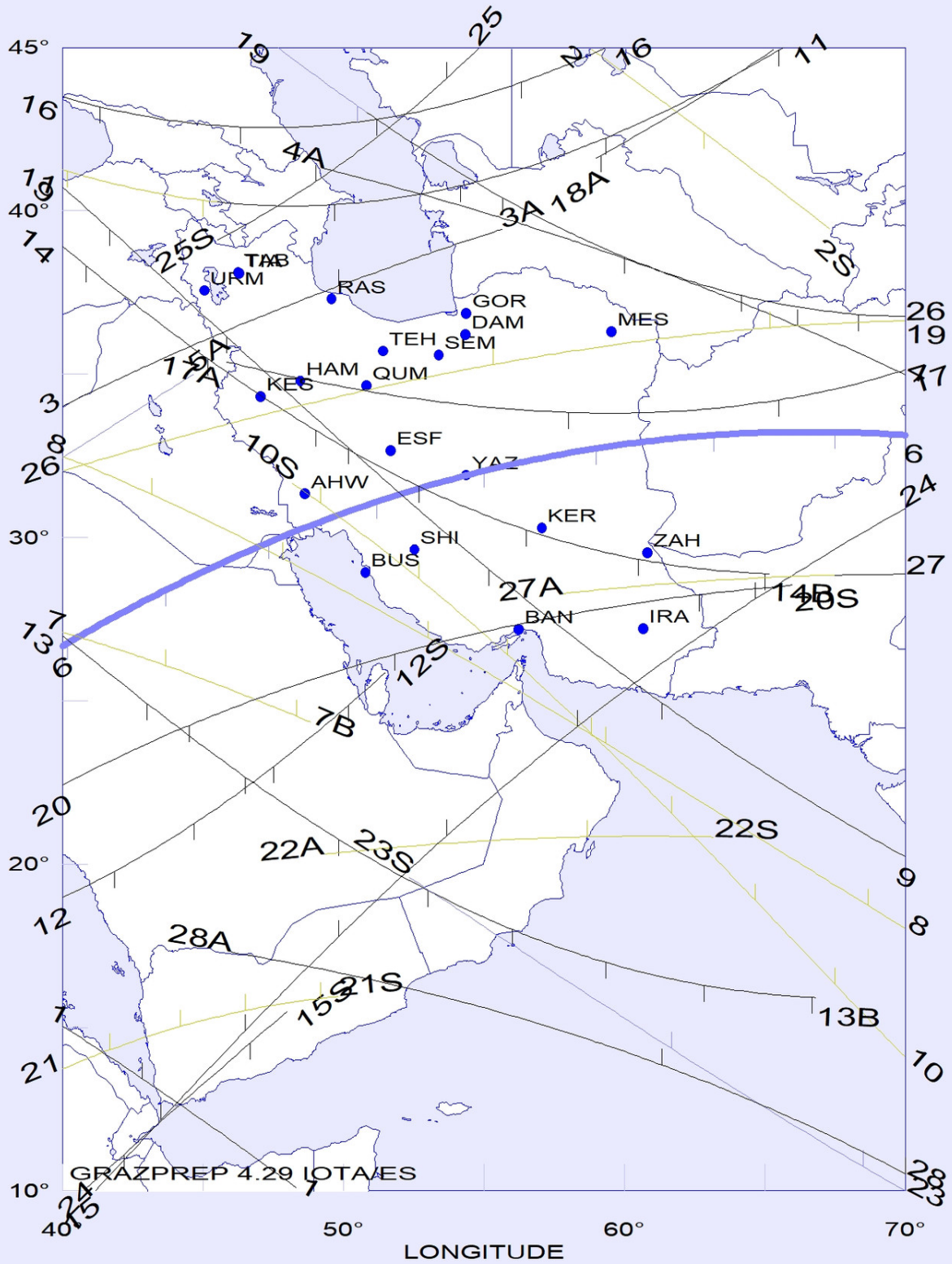


2021 Grazing Occultations Europe 2021 sel												GRAZPREP 4.27, IOTA/ES	
No.	M D	USNO	SAOPPM D	MAG	%SNL	L.	W.UT	LONG	LAT	STAR NAME	MAG1	MAG2	
1	Jan 02	ZC 1484	98955 C	3.5	84 -	N	20 25.1	4	34	eta Leonis NSV 04738	4.1	4.6	
2	Jan 16	ZC 3349	165321W	4.0	13+	S	16 14.6	40	34	tau Aquarii NSV 14329			
3	Feb 03	ZC 1941	139390	4.7	68 -	S	3 2.7	-4	65	74 Virginis NSV 06297			
4	Feb 07	ZC 2513	185401 K	4.2	22 -	N	7 25.9	-11	44	44 Ophiuchi NSV 08640	5.1	5.1	
5	Feb 08	ZC 2672	186841 w	2.8	14 -	N	7 29.0	-11	39	Kaus Borealis lambda Sagittarii			
6	Feb 14	ZC 5	128572 L	4.6	8+	S	15 32.3	22	56	33 Piscium BC Piscium	5.0	7.5	
7	Feb 16	ZC 249	110065	4.5	23+	S	19 53.8	-11	58	nu Piscium			
8	Apr 15	ZC 628	76532 K	4.9	11+	N	20 42.5	-11	58	omega 2 Tauri NSV 15938	5.0	7.0	
9	Apr 18	ZC 1030	78682W	3.1	34+	S	14 57.9	1	34	Mebstuta epsilon Geminorum			
10	Apr 19	ZC 1170	79653 A	3.6	45+	S	18 30.1	-11	36	kappa Geminorum	3.7	8.2	
11	Apr 19	ZC 1170	79653 A	3.6	45+	N	18 54.9	30	65	kappa Geminorum	3.7	8.2	
12	May 15	ZC 1030	78682W	3.1	14+	N	22 34.8	-9	65	Mebstuta epsilon Geminorum			
13	May 19	ZC 1484	98955 C	3.5	49+	N	16 49.7	-11	60	eta Leonis NSV 04738	4.1	4.6	
14	May 28	ZC 2750	187448 Y	2.0	91 -	N	22 26.4	17	53	Nunki sigma Sagittarii	2.9	2.9	
15	Jun 22	ZC 2307	184123	3.9	95+	N	18 6.9	9	47	Kow Kin omega 1 Scorpii			
16	Jun 22	ZC 2310	184135	4.3	95+	N	18 45.6	22	52	Kow Kin omega 2 Scorpii			
17	Jul 03	ZC 249	110065	4.5	37 -	S	3 4.8	-11	38	nu Piscium			
18	Jul 22	ZC 2750	187448 Y	2.0	98+	N	18 55.8	18	54	Nunki sigma Sagittarii	2.9	2.9	
19	Aug 17	ZC 2500	185320 J	3.3	73+	N	15 18.2	41	49	theta Ophiuchi	3.6	5.6	
20	Sep 02	ZC 1030	78682W	3.1	24 -	S	0 5.3	18	34	Mebstuta epsilon Geminorum			
21	Sep 03	ZC 1170	79653 A	3.6	16 -	S	2 43.6	-3	34	kappa Geminorum	3.7	8.2	
22	Sep 14	ZC 2650	186612	4.7	61+	S	19 12.4	-1	39				
23	Sep 27	ZC 709	76721 L	4.3	68 -	N	1 12.9	8	34	tau Tauri	4.9	6.4	
24	Sep 29	ZC 1030	78682W	3.1	48 -	S	10 47.6	22	65	Mebstuta epsilon Geminorum			
25	Oct 03	ZC 1484	98955 C	3.5	13 -	N	3 59.7	-11	53	eta Leonis NSV 04738	4.1	4.6	
26	Oct 05	ZC 1702	119035	4.0	2 -	N	1 49.5	42	52	nu Virginis			
27	Oct 08	ZC 2118	158840 V	2.8	7+	S	15 49.0	2	42	Zuben Elgenubi alpha 2 Librae	3.4	3.8	
28	Oct 24	ZC 656	76601 V	4.2	89 -	N	1 8.2	5	34	kappa Tauri NSV 01593	5.2	5.2	
29	Dec 11	ZC 3536	147042	4.4	57+	S	19 5.2	-11	54	30 Piscium YY Piscium	4.4	4.4	
30	Dec 26	ZC 1702	119035	4.0	59 -	N	5 35.1	-11	43	nu Virginis			



2021 Grazing Occultations India 2021 <= 5.0 mag. GRAZPREP 4.29, IOTA/ES											
No.	M D	USNO	SAOPPM D	MAG	%SNL	L.	W.UT	LONG LAT	STAR NAME	MAG1	MAG2
1	Jan 10	ZC 2513	185401 K	4.2	6-	S	23 47.3	83 29	44 Ophiuchi NSV 08640	5.1	5.1
2	Feb 03	ZC 2033	158427	4.2	59-	S	21 1.0	67 36	kappa Virginis NSV 20060		
3	Mar 19	ZC 628	76532 K	4.9	31+	S	13 22.2	72 16	omega 2 Tauri NSV 15938	5.0	7.0
4	Mar 22	ZC 1030	78682W	3.1	58+	N	6 56.1	89 33	Mebstuta epsilon Geminorum		
5	Apr 02	ZC 2513	185401 K	4.2	67-	N	17 60.0	86 24	44 Ophiuchi NSV 08640	5.1	5.1
6	Apr 17			1.4	25+	N	12 39.2	67 33	Mars		
7	Apr 18	ZC 1030	78682W	3.1	34+	S	17 28.7	67 20	Mebstuta epsilon Geminorum		
8	May 19	ZC 1484	98955 C	3.5	49+	N	18 56.8	67 22	eta Leonis NSV 04738	4.1	4.6
9	May 21	ZC 1702	119035	4.0	71+	S	16 38.6	67 17	nu Virginis		
10	Jun 30	ZC 3536	147042	4.4	59-	S	20 48.7	67 6	30 Piscium YY Piscium	4.4	4.4
11	Jul 22	ZC 2750	187448 Y	2.0	98+	S	20 35.4	76 5	Nunki sigma Sagittarii	2.9	2.9
12	Jul 26	ZC 3349	165321W	4.0	90-	N	18 42.9	67 34	tau Aquarii NSV 14329		
13	Aug 13	ZC 1941	139390	4.7	28+	N	14 0.3	68 22	74 Virginis NSV 06297		
14	Oct 09	ZC 2241	159442 V	4.8	13+	N	13 7.9	68 18	kappa Librae NSV 07200	5.8	5.8
15	Oct 12	ZC 2750	187448 Y	2.0	45+	N	16 8.7	67 6	Nunki sigma Sagittarii	2.9	2.9
16	Oct 16	ZC 3349	165321W	4.0	86+	S	20 2.9	67 29	tau Aquarii NSV 14329		
17	Oct 25	ZC 900	77775	4.8	77-	N	19 26.9	67 24	139 Tauri		
18	Nov 14	ZC 3536	147042	4.4	80+	S	11 52.0	78 29	30 Piscium YY Piscium	4.4	4.4
19	Nov 26	ZC 1484	98955 C	3.5	55-	S	21 46.6	82 36	eta Leonis NSV 04738	4.1	4.6
20	Nov 28	ZC 1702	119035	4.0	34-	S	21 25.8	67 29	nu Virginis		

Grazing Occultations Middle East 2021  $\leq 5.0$  mag.



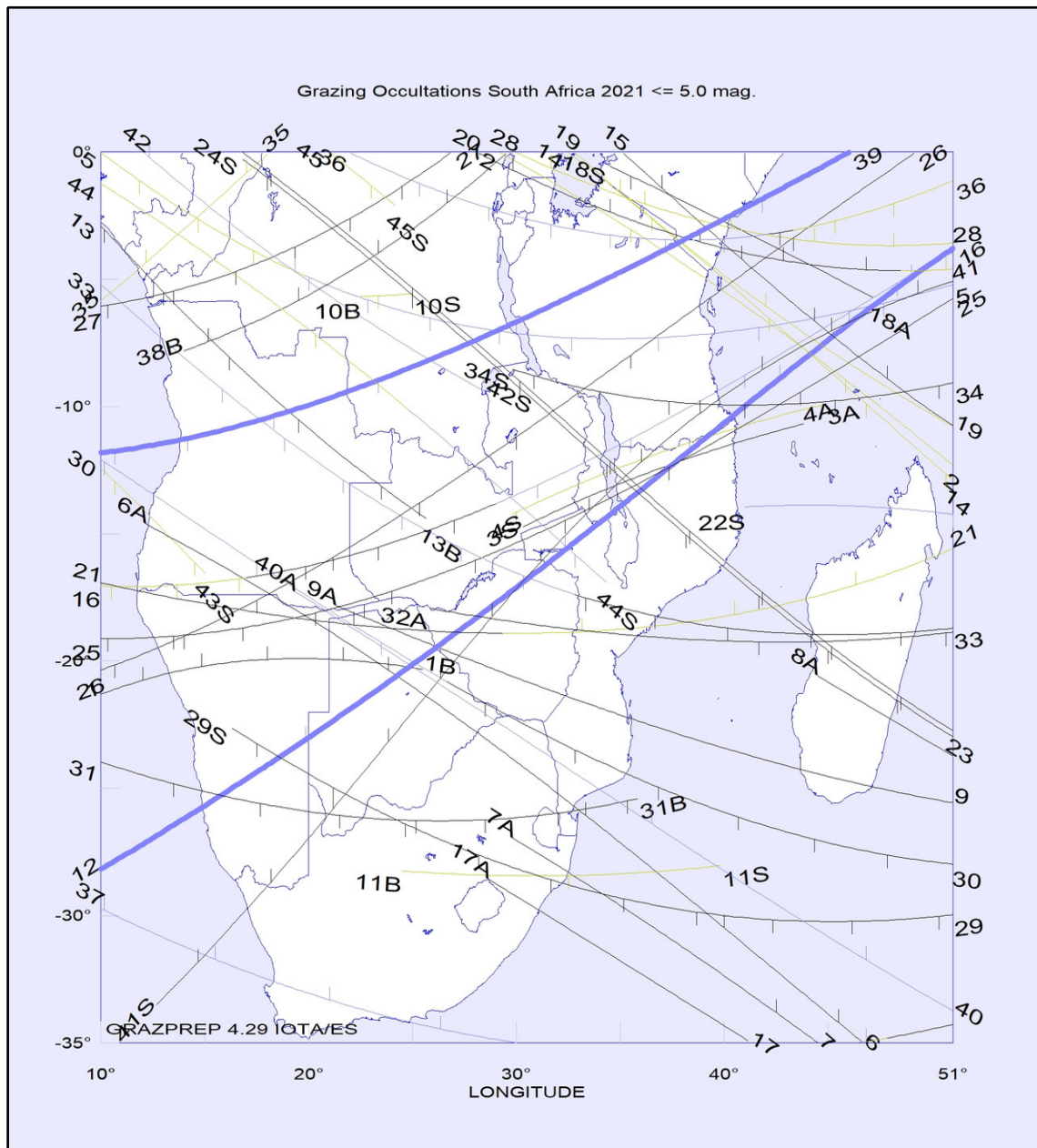
2021 Grazing Occultations Middle East 2021 <= 5.0 mag. <span style="float: right;">GRAZPREP 4.27, IOTA/ES</span>												
No.	M D	USNO	SAOPPM D	MAG	%SNL	L.	W.UT	LONG	LAT	STAR NAME	MAG1	MAG2
1	Jan 10	ZC 2376	184450	4.5	11-	S	2 27.4	40	15	omega Ophiuchi	4.5	4.5
2	Jan 10	ZC 2376	184450	4.5	11-	N	2 47.0	58	45	omega Ophiuchi	4.5	4.5
3	Jan 16	ZC 3349	165321W	4.0	13+	S	16 14.6	40	34	tau Aquarii NSV 14329		
4	Feb 03	ZC 2033	158427	4.2	59-	S	20 53.3	49	41	kappa Virginis NSV 20060		
5	Apr 04	ZC 2750	187448 Y	2.0	52-	S	7 32.4	40	32	Nunki sigma Sagittarii	2.9	2.9
6	Apr 17			1.4	25+	N	11 30.2	40	27	Mars		
7	Apr 17	ZC 882	77592 V	5.0	25+	S	16 1.6	40	27	132 Tauri	5.7	5.7
8	Apr 18	ZC 1030	78682W	3.1	34+	S	16 42.6	40	32	Mebstuta epsilon Geminorum		
9	May 19	ZC 1484	98955 C	3.5	49+	N	18 6.1	40	41	eta Leonis NSV 04738	4.1	4.6
10	May 21	ZC 1702	119035	4.0	71+	S	15 37.4	48	32	nu Virginis		
11	May 28	ZC 2750	187448 Y	2.0	91-	N	22 49.9	40	41	Nunki sigma Sagittarii	2.9	2.9
12	Jun 02	ZC 3349	165321W	4.0	52-	N	1 4.5	40	19	tau Aquarii NSV 14329		
13	Jun 22	ZC 2307	184123	3.9	95+	N	18 42.5	40	27	Kow Kin omega 1 Scorpii		
14	Jun 22	ZC 2310	184135	4.3	95+	N	19 8.5	40	39	Kow Kin omega 2 Scorpii		
15	Jun 28	ZC 3164	164520 U	4.5	86-	N	2 6.6	40	10	epsilon Capricorni	5.0	6.3
16	Jul 22	ZC 2750	187448 Y	2.0	98+	N	19 17.6	40	43	Nunki sigma Sagittarii	2.9	2.9
17	Jul 26	ZC 3349	165321W	4.0	90-	N	18 22.6	46	35	tau Aquarii NSV 14329		
18	Aug 02	ZC 628	76532 K	4.9	28-	N	20 40.5	59	42	omega 2 Tauri NSV 15938	5.0	7.0
19	Aug 17	ZC 2500	185320 J	3.3	73+	N	15 25.6	47	45	theta Ophiuchi	3.6	5.6
20	Sep 23	ZC 219	109926 w	4.8	96-	N	1 2.2	40	22	mu Piscium		
21	Sep 27	ZC 709	76721 L	4.3	68-	S	1 52.9	40	14	tau Tauri	4.9	6.4
22	Oct 05	ZC 1702	119035	4.0	2-	S	1 36.9	49	20	nu Virginis		
23	Oct 12	ZC 2721	187239 X	3.2	43+	S	9 51.1	52	20	phi Sagittarii	4.1	4.1
24	Oct 16	ZC 3349	165321W	4.0	86+	S	19 2.3	41	10	tau Aquarii NSV 14329		
25	Nov 14	ZC 5	128572 L	4.6	80+	S	13 43.9	45	39	33 Piscium BC Piscium	5.0	7.5
26	Nov 26	ZC 1484	98955 C	3.5	55-	S	21 1.3	40	32	eta Leonis NSV 04738	4.1	4.6
27	Nov 28	ZC 1702	119035	4.0	34-	S	21 23.0	58	28	nu Virginis		
28	Dec 01	ZC 1941	139390	4.7	14-	S	0 12.0	46	17	74 Virginis NSV 06297		

# Middle East



2021 Grazing Occultations North America 2021												GRAZPREP 4.27, IOTA/ES	
No.	M D	USNO	SAOPPM D	MAG	%SNL	L.	W.UT	LONG	LAT	STAR NAME	MAG1	MAG2	
1	Jan 01	ZC 1308	80378 V	4.7	95-	S	8 52.1	-115	52	Asellus Borealis gamma Cancri	5.5	5.5	
2	Jan 09	ZC 2307	184123	3.9	16-	S	17 49.2	-125	51	Kow Kin omega 1 Scorpii			
3	Jan 18	ZC 3536	147042	4.4	25+	S	5 28.4	-125	45	30 Piscium YY Piscium	4.4	4.4	
4	Jan 21	ZC 327	110408 K	4.4	52+	S	4 38.1	-125	45	xi 1 Ceti NSV 00749	5.3	5.3	
5	Feb 06	ZC 2376	184450	4.5	32-	N	8 52.0	-84	43	omega Ophiuchi	4.5	4.5	
6	Feb 13	ZC 3349	165321W	4.0	2+	S	1 18.0	-118	44	tau Aquarii NSV 14329			
7	Feb 20	ZC 628	76532 K	4.9	54+	N	6 17.4	-125	29	omega 2 Tauri NSV 15938	5.0	7.0	
8	Feb 25	ZC 1308	80378 V	4.7	93+	S	1 6.7	-113	50	Asellus Borealis gamma Cancri	5.5	5.5	
9	Mar 02	ZC 1941	139390	4.7	88-	S	9 49.1	-125	41	74 Virginis NSV 06297			
10	Apr 08	ZC 3349	165321W	4.0	12-	N	12 34.3	-117	39	tau Aquarii NSV 14329			
11	Apr 24	ZC 1702	119035	4.0	88+	N	6 36.5	-120	54	nu Virginis			
12	May 15	ZC 1030	78682W	3.1	14+	S	22 47.4	-76	39	Mebstata epsilon Geminorum			
13	May 17	ZC 1170	79653 A	3.6	23+	S	1 30.1	-117	39	kappa Geminorum	3.7	8.2	
14	Jun 12	ZC 1030	78682W	3.1	3+	N	4 30.3	-109	55	Mebstata epsilon Geminorum			
15	Jun 15	ZC 1484	98955 C	3.5	27+	N	23 13.2	-104	55	eta Leonis NSV 04738	4.1	4.6	
16	Jun 25	ZC 2750	187448 Y	2.0	99-	N	10 3.6	-125	45	Nunki sigma Sagittarii	2.9	2.9	
17	Jun 29	ZC 3349	165321W	4.0	75-	N	9 33.8	-110	25	tau Aquarii NSV 14329			
18	Jul 20	ZC 2310	184135	4.3	79+	N	3 15.5	-121	36	Kow Kin omega 2 Scorpii			
19	Jul 25	ZC 3164	164520 U	4.5	98-	N	12 21.8	-123	25	epsilon Capricorni	5.0	6.3	
20	Aug 19	ZC 2750	187448 Y	2.0	86+	N	2 34.1	-125	39	Nunki sigma Sagittarii	2.9	2.9	
21	Aug 23	ZC 3349	165321W	4.0	99-	N	4 1.7	-118	49	tau Aquarii NSV 14329			
22	Sep 13	ZC 2500	185320 J	3.3	50+	N	20 8.0	-82	34	theta Ophiuchi	3.6	5.6	
23	Sep 15	ZC 2721	187239 X	3.2	65+	S	6 39.5	-125	34	phi Sagittarii	4.1	4.1	
24	Oct 12	ZC 2650	186612	4.7	37+	S	1 40.7	-83	25				
25	Oct 24	ZC 709	76721 L	4.3	88-	N	8 56.6	-125	50	tau Tauri	4.9	6.4	
26	Oct 30	ZC 1484	98955 C	3.5	33-	S	14 7.1	-125	31	eta Leonis NSV 04738	4.1	4.6	
27	Oct 30	ZC 1484	98955 C	3.5	33-	N	14 45.2	-86	55	eta Leonis NSV 04738	4.1	4.6	
28	Nov 01	ZC 1702	119035	4.0	15-	S	12 1.7	-125	26	nu Virginis			
29	Nov 01	ZC 1702	119035	4.0	15-	N	12 36.1	-87	55	nu Virginis			
30	Nov 03	ZC 1941	139390	4.7	3-	N	13 25.6	-118	48	74 Virginis NSV 06297			
31	Nov 03			-0.8	2-	S	19 4.3	-118	55	Mercury			
32	Nov 09	ZC 2914	188778 V	4.8	32+	S	22 3.1	-76	36	Terebellum 60 Sagittarii	5.8	5.8	
33	Nov 12	ZC 3349	165321W	4.0	65+	N	23 57.9	-96	25	tau Aquarii NSV 14329			
34	Dec 31	ZC 2359	184382 D	5.0	8-	S	12 26.9	-82	54	rho Ophiuchi			

# North America



2021 Grazing Occultations South Africa 2021 <= 5.0 mag.											GRAZPREP 4.27, IOTA/ES	
No.	M D	USNO	SAOPPM D	MAG	%SNL	L.	W.UT	LONG	LAT	STAR NAME	MAG1	MAG2
1	Jan 23	ZC 628	76532 K	4.9	77+	S	20 43.2	10	-21	omega 2 Tauri NSV 15938	5.0	7.0
2	Feb 05	ZC 2322	159764 Y	4.1	34-	N	23 57.0	29	0	Jabbah nu Scorpii	4.9	6.9
3	Feb 13	ZC 3425	146620 K	4.4	4+	N	16 30.9	30	-14	psi 2 Aquarii	5.4	5.4
4	Feb 13	ZC 3428	146635 A	5.0	4+	S	16 31.2	30	-15	psi 3 Aquarii NSV 14491	5.2	11.2
5	Mar 05	ZC 2302	159682 H	2.6	60-	N	4 13.3	10	0	Graffias beta 1 Scorpii	3.2	4.2
6	Apr 01	ZC 2376	184450	4.5	76-	S	20 54.7	12	-15	omega Ophiuchi	4.5	4.5
7	Apr 02	ZC 2523	185470	4.8	66-	S	20 14.0	30	-27	51 Ophiuchi NSV 09037		
8	Apr 04	ZC 2864	188337 A	4.6	44-	S	21 22.8	44	-21	52 Sagittarii	4.7	9.2

(Continued on next page)

2021 Grazing Occultations South Africa 2021 <= 5.0 mag. <span style="float: right;">GRAZPREP 4.27, IOTA/ES</span>												
No.	M D	USNO	SAOPPM D	MAG	%SNL	L.	W.UT	LONG	LAT	STAR NAME	MAG1	MAG2
9	Apr 07	ZC 3164	164520 U	4.5	22-	S	0 59.9	21	-18	epsilon Capricorni	5.0	6.3
10	Apr 07	ZC 3175	164593	4.7	22-	N	4 18.1	22	-6	kappa Capricorni		
11	Apr 09	ZC 3428	146635 A	5.0	8-	N	3 23.6	24	-28	psi 3 Aquarii NSV 14491	5.2	11.2
12	Apr 17			1.4	25+	S	10 18.7	10	-28	Mars		
13	Apr 24	ZC 1773	119341 V	5.0	93+	N	22 19.8	10	-3	16 Virginis	5.8	5.8
14	Apr 28	ZC 2302	159682 H	2.6	95-	N	19 44.5	32	0	Graffias beta 1 Scorpii	3.2	4.2
15	Apr 28	ZC 2307	184123	3.9	95-	S	21 15.7	35	0	Kow Kin omega 1 Scorpii		
16	May 01	ZC 2672	186841 w	2.8	78-	N	3 18.4	10	-17	Kaus Borealis lambda Sagittarii		
17	May 01	ZC 2809	187882 Q	4.9	70-	S	20 2.5	28	-29	psi Sagittarii	6.2	6.2
18	May 13	ZC 709	76721 L	4.3	3+	N	15 39.3	34	-1	tau Tauri	4.9	6.4
19	May 19	ZC 1484	98955 C	3.5	49+	S	19 6.2	32	0	eta Leonis NSV 04738	4.1	4.6
20	May 28	ZC 2750	187448 Y	2.0	91-	S	22 16.7	28	0	Nunki sigma Sagittarii	2.9	2.9
21	Jun 01	ZC 3349	165321W	4.0	52-	S	23 54.5	10	-17	tau Aquarii NSV 14329		
22	Jun 17	ZC 1651	99587 O	3.9	43+	N	10 11.7	41	-14	Tsze Tseang iota Leonis	4.0	6.7
23	Jun 22	ZC 2302	159682 H	2.6	94+	N	16 58.6	16	0	Graffias beta 1 Scorpii	3.2	4.2
24	Jun 22	ZC 2303	159683 B	4.8	94+	N	16 58.8	16	0		5.2	7.6
25	Jun 24	ZC 2672	186841 w	2.8	100-	N	23 49.4	10	-19	Kaus Borealis lambda Sagittarii		
26	Jun 26	ZC 2864	188337 A	4.6	98-	N	1 28.3	10	-20	52 Sagittarii	4.7	9.2
27	Jun 28	ZC 3164	164520 U	4.5	86-	N	0 19.2	10	-6	epsilon Capricorni	5.0	6.3
28	Jul 22	ZC 2750	187448 Y	2.0	98+	S	18 46.7	30	0	Nunki sigma Sagittarii	2.9	2.9
29	Aug 17	ZC 2513	185401 K	4.2	74+	N	16 37.4	16	-23	44 Ophiuchi NSV 08640	5.1	5.1
30	Aug 18	ZC 2672	186841 w	2.8	83+	N	15 30.8	10	-12	Kaus Borealis lambda Sagittarii		
31	Aug 19	ZC 2864	188337 A	4.6	91+	N	18 22.4	10	-24	52 Sagittarii	4.7	9.2
32	Aug 23	ZC 3428	146635 A	5.0	98-	N	17 31.7	26	-18	psi 3 Aquarii NSV 14491	5.2	11.2
33	Sep 12	ZC 2307	184123	3.9	37+	N	14 21.6	10	-5	Kow Kin omega 1 Scorpii		
34	Sep 12	ZC 2310	184135	4.3	37+	N	15 56.9	30	-9	Kow Kin omega 2 Scorpii		
35	Sep 27	ZC 709	76721 L	4.3	68-	S	0 16.6	10	-6	tau Tauri	4.9	6.4
36	Oct 12	ZC 2750	187448 Y	2.0	45+	N	13 50.9	22	0	Nunki sigma Sagittarii	2.9	2.9
37	Oct 12	ZC 2750	187448 Y	2.0	45+	S	13 50.6	10	-30	Nunki sigma Sagittarii	2.9	2.9
38	Oct 16	ZC 3349	165321W	4.0	86+	S	17 37.8	14	-8	tau Aquarii NSV 14329		
39	Dec 04			-1.1	0+	N	13 38.4	10	-12	Mercury		
40	Dec 06	ZC 2750	187448 Y	2.0	6+	S	6 12.7	19	-17	Nunki sigma Sagittarii	2.9	2.9
41	Dec 13	ZC 219	109926 w	4.8	76+	S	18 15.2	12	-34	mu Piscium		
42	Dec 24	ZC 1484	98955 C	3.5	78-	S	6 30.5	12	0	eta Leonis NSV 04738	4.1	4.6
43	Dec 29	ZC 2033	158427	4.2	27-	N	4 18.7	10	-12	kappa Virginis NSV 20060		
44	Dec 31	ZC 2307	184123	3.9	9-	N	3 51.9	10	-1	Kow Kin omega 1 Scorpii		
45	Dec 31	ZC 2310	184135	4.3	9-	N	4 17.5	21	0	Kow Kin omega 2 Scorpii		

# The Shelyak TimeBox - A Device Allowing Multi-Mode Accurate UTC Time Recordings for Digital Video Cameras

Cesar Valencia Gallardo · TimeBox UTC · Paris · France · info@timeboxutc.com  
Dave Gault · WSAAG · Hawkesbury Heights · Australia · davegault@bigpond.com  
Thierry Midavaine · Club Eclipse · Paris · France · thierrymidavaine@sfr.fr  
Hristo Pavlov · IOTA/ES · Karlovo · Bulgaria · hristo\_dpavlov@yahoo.com

**ABSTRACT:** The Shelyak TimeBox has just been released as a multi-mode, accurate, modular and portable solution for UTC timing using digital video cameras in a *Windows* environment. The goal of this article is to show the results of independent testing of the Shelyak TimeBox using described methods that measure the accuracy of UTC timestamped recordings for both featured computer and trigger modes. The results of the tests and recordings presented in this article showed that the Shelyak TimeBox was able to allow accurate UTC timestamped recordings using digital cameras up to the millisecond (ms) precision. The modular design of the Shelyak TimeBox separates the UTC timestamping from the recording camera, allowing the use of the last-generation, sensitive and low noise CCD, EMCCD and CMOS image sensors for occultations and other astronomical phenomena requiring precise UTC timestamping.

## Introduction

The timestamping of astronomical occultations and other astronomical phenomena need to be done in an absolute time scale in order to allow collaborations between different observers around the world. The timescale chosen is the Coordinated Universal Time (UTC) that is the primary time standard regulating clocks and time [1]. Stellar occultation by Solar System Objects (SSO) is a proven method used to determine the size, 3D shape, topology and accurate positioning of asteroids including their satellites [2]; in addition, stellar occultations are used to improve astrometry of asteroid orbits by linking their position to the *Gaia* coordinates of a star at event epoch [3], to measure occulted star size, to detect multiple star systems, to detect asteroid satellites, to produce accurate TNOs ephemeris [4], to provide information of the atmospheric pressure of TNOs and planets [5], and recently, to discover the presence of rings around minor planets of the outer solar system [6].

Most amateur astronomers use a timing system that stamps the UTC time in every frame of an analogue video recording using the Composite Video Baseband Signal (CVBS) standard and devices that use either a radio clocking signal as DCF77 or a Global Navigation Satellite System (GNSS) receiver (Black Box, Kiwi device, TIM10, IOTA-VTI). This system was validated by the International Occultation Timing Association (IOTA) community for years and used by many observers for almost twenty years [7].

Most observations are still made using analogue video cameras coupled to analogue-to-digital converters producing digital DVI

or SER files. However many observers wish to use the many advances in image quality that new digital video cameras offer, including bit depth increasing from 8 bits to 12-16 bits among others. The last generation of the most sensitive and low noise CCD, EMCCD and CMOS image sensors are embedded in digital cameras. CMOS image sensors are digital as the sensor chip itself produces a digital output compared to the analogic one produced by the CCD arrays. Last generation CMOS image sensors possess sensitivity and noise levels comparable or above to those of the best CCD sensors, without its major limitations like the low frame rate and high costs of production [8]. The evolution of CMOS image sensor capabilities is likely replacing the CCD sensors thus favouring the development of affordable highly sensitive/low noise digital video devices now and in the near future.

In order to use digital cameras for the recording of astronomical occultations, these systems' UTC timing has to be accurate and robust. Some options like the QHY174M-GPS camera [9] and systems such as ADVS and others [10, 11, 12] are capable to meet the needed accuracy but they are either not widely available or limited in the choice of image sensors and cameras for the amateur community. A recent article by Pavlov & Gault [13], showed that there is a way to accurately correct (better than  $\pm 15$  ms in 99 % of the time) the PC system date/time using the *Meinberg NTP* software [14]. The method described by Pavlov & Gault requires an internet ADSL connection, has an initial time to achieve  $\pm 15$  ms UTC synchronization within approximately 1-2 hours after a cold start, and exposes to similar times to recovery from a rare erroneous single shift during the synchronization [13].

Achieving accurate timing with a PC is challenging because it depends on many factors like the variability in the internal RTC clock, the tolerance (ppm) and variation with the temperature of CPU-clocking crystal oscillators, the presence of multiple motherboard CPUs in modern computers, high priority system interruptions by the operating system, different date/time management depending on the version of the operating systems among other factors [13]. A way to be sure that the *Windows* time will not be affected by multi-core and power management is to verify that the time is based on the crystal oscillator on the motherboard. As described in Pavlov & Gault, a method to verify these conditions is to check that the CPU used supports a feature called Invariant TSC and that this feature is supported by the *Windows* OS version used [13, 15]. The majority of *Windows 7* operating systems and above support Invariant TSC, but it is preferable to use *Windows 10* because of the additional improvements made to its kernel and task scheduler that directly affect the accuracy of the system date/time [13, 16].

In February 2020, the Shelyak TimeBox [17] in Figure 1 was released as an accurate and portable solution for UTC timing using digital video cameras in a *Windows* environment. The Shelyak TimeBox is designed to allow accurate timing of astronomical phenomena using digital video devices. It provides the base for several modular set-ups that can be used with a wide variety of astronomical hardware. The Shelyak TimeBox recovers the UTC time from GPS satellites and synchronizes the recordings using three different modes:

**LED firing:** This mode allows inserting the UTC time directly and optically in the video frame stream by firing a LED at each UTC-second. The accuracy of the rise of the LED firing was measured against the UTC-OP of the SYRTE at the *Observatoire de Paris* [18] to be delayed by +10  $\mu$ s UTC.

**Computer Synchronization:** This mode allows the synchronization of a PC using a *Windows* operating system internal date/time with the UTC reference delivered and updated by the TimeBox device and proprietary software. Then computer synchronization mode

allows the recorded frames to be accurately timestamped by the PC with the UTC-synchronized system date/time. The accuracy of the recordings made with the Shelyak TimeBox in computer mode was measured by the team of Pr. Sicardy. Their findings presented in Dr. Leiva's doctoral thesis showed that the accuracy of the recorded frames stayed below the resolution limit of the test defined at  $\pm 20$  ms UTC [19]. The accuracy of this method was also measured in-house by comparing the difference between timestamps of the recorded frames against the firing of a GPS 1PPS, and found to be approximately  $\pm 5$  ms UTC (>95%, 2 standard deviations) at the resolution limit of the sampling method ["Technical Datasheet and Controls", 20].

**Trigger:** In this mode the Shelyak TimeBox is able to trigger the camera driving the exposure by emitting a series of TTL logic square UTC-timed pulses through a BNC port at a frequency chosen between 0.1 and 24 Hz. In this mode, the Shelyak TimeBox is also able to synchronize the internal PC-clock to ease data reduction and produces a log containing the list of the pulses. The accuracy of this method was measured in-house by comparing the difference between the Shelyak TimeBox pulses against the firing of a GPS 1PPS using an oscilloscope, and found to be better than 1 ms UTC (data not shown).

Using the Shelyak TimeBox in both LED firing or Computer Synchronization requires a simple USB connection as the power needed is drawn from the USB port. On the other hand, Trigger mode needs additional power for firing the pulses sent into the I/O port of the camera. An additional 12 V power supply has to be connected into the dedicated Shelyak TimeBox 12 V DC-input when using the Trigger mode (Figure 1).

The goal of this article is to show the results of the independent testing of the Shelyak TimeBox using described methods [13, 21] that measure the accuracy of UTC timestamped recordings for both computer synchronization and trigger modes, to assess the accuracy of the timestamping when using different cameras and acquisition software, and to measure the accuracy of the PC date/time synchronization on long periods of time.



Figure 1. The Shelyak TimeBox, a device designed for accurate UTC time recordings with digital video cameras.

A - Shelyak TimeBox face A.  
B - Shelyak TimeBox face B, display the (left to right) USB-B port, GPS antenna SMA port, TTL trigger output port and 12 V DC-input for trigger mode.

## Materials and Methods

### Windows 10 and Windows 7 operating system time drift

A dual installation of *Microsoft Windows 10 Professional* and *Windows 7 Professional Service Pack 1* operating systems was done on a PC AMD FX-8350 4 GHz, 16Gb RAM system. The *TimeBox 1.8.2 XS* software version was installed in *Windows 10*, while the *TimeBox 1.8.2 Legacy* version in *Windows 7* ["Software and firmware", 17]. Each operating system was booted and a 15 minutes recording of the system's time drift compared to the Shelyak TimeBox timestamps done during the calibration routine for each operating system. The system date/time in *Windows 10* was read using the `GetSystemTimePreciseAsFileTime` function, and the system date/time in *Windows 7* was read using the `GetSystemTime` function. Linear fits for both recordings were calculated using the polynomial curve fitting "polyfit" (degree = 1) function in Matlab (R2020a).

### Digital cameras with Shelyak TimeBox in Computer mode compared to SEXTA

A *Windows 10* 64-bits system (AMD FX-8350 4 GHz, USB2) was permanently synchronized using a Shelyak TimeBox in computer mode for at least 15 min using default synchronization parameters using the *TimeBox 1.8.2 XS* software version. Following, the screen of a SEXTA [21] device was recorded by three different digital cameras a Basler 640-100gm GigE Global shutter, a ZWO ASI183MM-Pro USB3 Rolling shutter and a Basler acA3088-57um USB3 Rolling shutter at 4, 10, 20 and 40 FPS for two min each. A constant time offset for each camera was determined and the frames timestamp corrected with the corresponding offset. All acquisitions were done using *AiryLab's Genika Astro x64bits* (Release 2.13.5.8) as recording software [22] and the frames saved as a single SER file for each acquisition. Timestamps were recovered from the SER image header and compared to the SEXTA's optical timestamps using the provided *SEXTAreader* software [21]. In the case of rolling shutter cameras, the timestamps were corrected according to this formula: reading time of the line (tRow) x number of the line where we find the object to be dated (Row), the timestamp corresponds at the time when the camera records the first line. The reading time of the line (tRow) depends on the camera and can be obtained by:

$$tRow = (1/FPS_{max})/TotalRow$$

FPS<sub>max</sub> = Maximum frame rate (FPS)

TotalRow = Total number of lines read at that max FPS

Mean, STD and linear regression were calculated for each acquisition. Linear regressions were calculated using the polynomial curve fitting "polyfit" (degree = 1) function in Matlab (R2020a).

### Acquisition software with Shelyak TimeBox in Computer mode compared to SEXTA

A *Windows 10* 64-bits system laptop (Lenovo ThinkPad Intel i5 Core i5-540M, 4GB DDR3 RAM, USB2.0) was permanently synchronized using a Shelyak TimeBox in computer mode for at

least 15 minutes using default synchronization parameters using the *TimeBox 1.8.2 XS* software version. Following, the LED matrix screen of a SEXTA [21] device was recorded using a Basler 640-100gm GigE camera with three different acquisition software:

*AiryLab Genika*, *SharpCap* and *PRISM* at 4, 10, 20 and 40 FPS frequencies for 2 min each. A constant latency time offset for each camera was determined and the frames timestamp corrected with the related offset. The acquisitions were done using *AiryLab's Genika Astro x64bits* (Release 2.13.5.8) [22], *SharpCap* (3.2.6101.0) [23], and *PRISM* (v10) [24] and the frames saved as a single SER file for each acquisition. Timestamps were recovered from the SER image header and compared to the SEXTA's optical timestamps using the provided *SEXTAreader* software [21]. Mean delay and variance (standard deviation) for each frame recorded at all acquisition rates were calculated for each acquisition software and compared using a One-way ANOVA post-hoc test using Matlab's (R2020a) "anova1" and "multcompare" functions.

### Shelyak TimeBox Trigger mode compared to SEXTA

A Shelyak TimeBox in trigger mode was used to produce UTC-synchronized TTL pulses used to trigger frame acquisitions on a Basler 640-100gm GigE digital camera recording the LED matrix screen of a SEXTA [21] device at 1, 2, 4, 8, 10, 15, 20 and 24 FPS for two min each. All acquisitions were done using the *TimeBox 1.8.2 XS* software version in a *Windows 10* 64-bits system laptop (Lenovo ThinkPad Intel i5 Core i5-540M, 4GB DDR3 RAM, USB2.0). *AiryLab's Genika Astro x64* (Release 2.13.5.8) was used as recording software and the frames saved in a single SER file for each acquisition. Frames were set to be triggered using the built-in external trigger of the camera by checking the *Genika's* "HW trigger" case as shown in the user manual page 25 [22]. A standard 12 V DC power plug was connected to the dedicated Shelyak TimeBox 12 V DC-input as described in the user manual page 14 [22]. The resulting SER video timestamps were re-synchronized with the acquisition TimeBox log using the *AiryLab SER Toolbox* (v 2.0.1.0) included with *Genika*, as detailed in the Shelyak TimeBox user manual pages 20-21 [25]. The timestamps of the re-synchronized SER files were recovered from the frame header and compared to the SEXTA's optical timestamps using the provided *SEXTAreader* software [21]. The mean, STD and linear regression were calculated for each acquisition. Linear regressions were calculated using the polynomial curve fitting "polyfit" (degree = 1) function in Matlab (R2020a).

### Shelyak TimeBox in computed mode compared to IOTA-VTI/ OccuRec

*OccuRec* [26] was used to survey the synchronization of the internal clock of a *Windows 10* 64-bits system (Toshiba Qosmio F750, Intel processor i7, 8Gb RAM and Samsung EVO 850 SSD hard drive) to the Coordinated Universal Time (UTC) for 4 h, 6 h, and 24 h at 24 timestamps/second as described in Pavlov & Gault [13]. The computer internal clock was permanently synchronized using a Shelyak TimeBox in computer mode with default synchronization parameters; different "Time correction" modes were tested: Slow, Medium and Fast, the synchronization was done using the *TimeBox 1.8.2 XS* software version. *OccuRec* recorded the system time using

the *Windows 10* `GetSystemTimePreciseAsFileTime` function against a time reference provided by the IOTA-VTI obtained by automatically reading the OCR timestamp for every single frame during the recording (40 ms, PAL). Matlab (R2020a) was used to calculate a one-minute (1440 timestamps window) moving mean of the delay (ms) between the Shelyak TimeBox and the IOTA-VTI obtained by using the “movmean” function, and linear regressions by using the polynomial curve fitting “polyfit” (degree = 1) function. The frequency distribution of the delays between the Shelyak TimeBox and the IOTA-VTI were represented in a histogram. The statistical measures of the mean of the delay (ms), STD, minimum and number of measures (n) are shown for each recording.

## Results

In order to determine the more accurate method for reading the system date/time in a *Windows* PC, a dual installation of *Microsoft Windows 10 Professional* and *Windows 7 Professional Service Pack 1* operating systems was done on a single PC (see chapter *Materials and Methods*). A dual installation allowed to prevent bias in the recordings due to hardware variability [13]. Each operating system was booted individually, two installations of the Shelyak TimeBox software were done in each operating system: *TimeBox 1.8.2 XS* version in *Windows 10* and the *TimeBox 1.8.2 Legacy* version in *Windows 7*. The *TimeBox XS* version is compatible with *MS Windows 8* system and up and uses the `GetSystemTime-AsPreciseAsFileTime` function to read the system date/time, while the *TimeBox Legacy* version is compatible with *MS Windows XP* systems and above and uses the `GetSystemTime` function to read the system date/time. After installing the corresponding *TimeBox*

software, the same Shelyak TimeBox device was connected to the computer USB2 and the antenna was placed in an open-sky location to allow the internal GPS of the Shelyak TimeBox to be fixed. After fixation one mandatory calibration routine was done for each operating system. A calibration file was produced after each calibration routine; this file contains 15 min recordings of the system’s date/time drift compared to the Shelyak TimeBox UTC timestamps.

As shown in Figure 2, both functions `GetSystemTimePreciseAsFileTime` and `GetSystemTime` measure a similar system time drift as expected when measuring on the same computer. `GetSystemTimePreciseAsFileTime` measured a slope of 2.02 ms/min while `GetSystemTime` measures a slope of 1.77 ms/min (Figure 2A). On the other hand, we observed that the variance of the date/time measures was significantly increased when using the *Windows 7* `GetSystemTime` function compared to the *Windows 10* `GetSystemTimePreciseAsFileTime` function (Figure 2B). The subtraction of the slope during the time drifts was used to measure the variances  $\pm 2.4$  and  $\pm 10$  ms UTC (>95%, 2 standard deviations) for `GetSystemTimePreciseAsFileTime` and `GetSystemTime` respectively (Figure 2B). The increase in the variance was also reflected on the linear correlation coefficient measured at  $r = 0.51$  and  $r = 0.96$  for `GetSystemTime` compared to `GetSystemTime-PreciseAsFileTime` respectively (Figure 2A). These results show that the *Windows 10* `GetSystemTimePreciseAsFileTime` is better suited to read the system date/time compared to the *Windows 7* `GetSystemTime` function. Recent developments on the system date/time reading were done when releasing *Windows 8* to provide microsecond resolution of the timestamps when using the `GetSystemTimePreciseAsFileTime` function [13, 27, 28]. For this

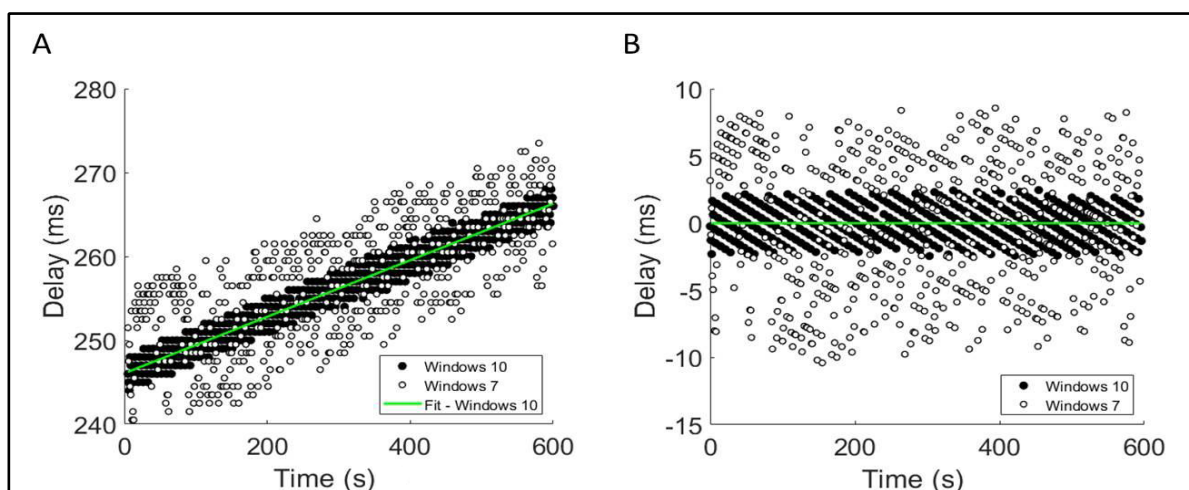


Figure 2A, B. *Windows 10* `GetSystemTimePreciseAsFileTime` function improves system’s date/time reading.

15 minutes recordings of the system’s date/time drift compared to the Shelyak TimeBox timestamps. The system’s date/time drift was read either in *Windows 10*’s using `GetSystemTimePreciseAsFileTime` function (● filled circles) or in *Windows 7* using `GetSystemTime` function (○ empty circles).

A) Linear fits for both measurements were calculated for *Windows 10* `GetSystemTimePreciseAsFileTime` with a slope = 2.02 ms/min and a  $r = 0.96$  represented in green, and *Windows 7* `GetSystemTime` with a slope = 1.77 ms/min and a  $r = 0.51$ .

B) Subtraction of the slopes during the system date/time drifts were used to measure the standard deviations  $\pm 1.2$  and  $\pm 5.0$  ms UTC when using `GetSystemTimePreciseAsFileTime` and `GetSystemTime` function respectively.

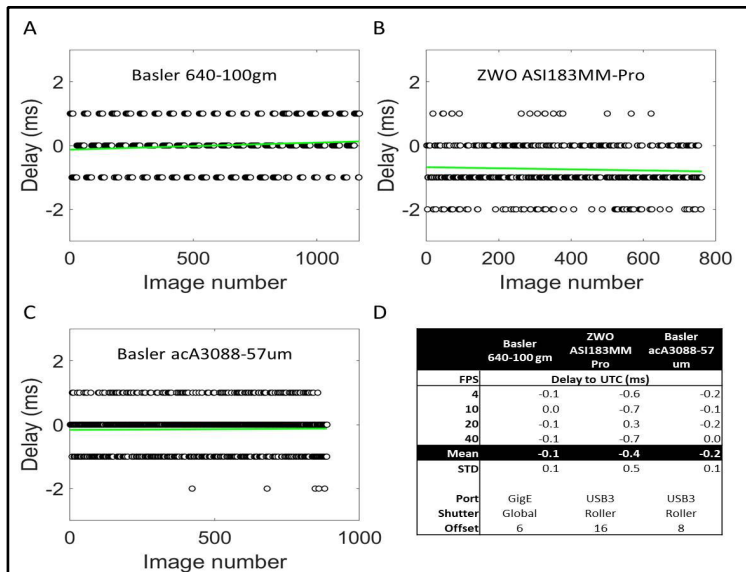


Figure 3A-D. Shelyak TimeBox in Computer mode allows the accurate timestamping of recordings for both global/rolling shutter digital cameras.

Different digital cameras were used to record a SEXTA device for 2 minutes at different acquisition frequencies; the system's date/time was synchronized using a Shelyak TimeBox in Computer mode and Airylab's Genika as acquisition software. Representative result of the Delay (ms) between the frames timestamps and the SEXTA optical timestamps for the duration of the recording (10 FPS) are shown:

- A) Basler 640-100gm GigE Global shutter camera
- B) ZWO ASI183MM-Pro USB Rolling shutter camera
- C) Basler acA3088-57um USB Rolling shutter camera.

The results of the measures at different acquisition rates for all three cameras are shown in D, where the mean Delay (ms) for each acquisition is corrected for the constant time offset (ms) of the recording.

reason, all the following tests were performed on Windows 10 systems using the TimeBox 1.8.2 XS software version that uses the GetSystemTimePreciseAsFileTime function to read the system date/time.

In order to measure the UTC timestamp accuracy of frames recorded by a PC permanently synchronized using a Shelyak TimeBox in computer mode, the screen of a SEXTA [21] device was recorded using three global or rolling shutter cameras: Basler 640-100 gm, ZWO ASI183MM-Pro and Basler acA3088-57um. The recordings were done at different acquisition frequencies for 2 min using Airylab Genika as acquisition software as described in Materials and Methods. The delay between each frame timestamp was subtracted from the SEXTA optical timestamp read by the provided SEXTAreader software; representative results for an acquisition frequency of 10 FPS are shown in Figure 3A, 3B and 3C for each camera.

The results of the measurements at different acquisition rates for all three cameras are shown in Figure 3D. The analysis of the mean delay for each camera and acquisition frequencies show that there is a constant time offset for all acquisition frequencies for each camera (Figure 3D, Offset). A constant time offset was observed when recording with digital systems [13], to measure it the Shelyak TimeBox possesses a built-in LED and a procedure that allows measuring this offset described on page 17 of the user manual [25]. The constant time offset for the Basler 640-100 gm, ZWO ASI183MM-Pro and Basler acA3088-57um were measured at +6, +16 and +8 ms respectively. The constant time offsets were used to correct the frames timestamps for each camera at any given acquisition frequency. The results in figure 3D show that the corrected mean of the UTC-timestamps of the recordings done with a Basler 640-100 gm, a ZWO ASI183MM-Pro and a Basler acA3088-57um cameras measured at -0.1, -0.4 and 0.2 ms with standard deviations of  $\pm 0.1$ ,  $\pm 0.5$  and  $\pm 0.1$  respectively. It is

important to note that the recording made with the rolling shutter cameras needs to be corrected as described in Materials and Methods; indeed the rolling shutter mode induces a drift of the exposure start and end through the array [8]. These results show that the accuracy of the UTC timestamps recorded with these digital systems permanently synchronized with a Shelyak TimeBox in computer mode is better than 1 ms with mean standard deviations of less than  $\pm 0.5$  ms. It is important to remember that the configuration of the SEXTA used during these recordings offers a temporal resolution down to 2 ms referred to UTC [21].

To evaluate the impact of using different acquisition software on the accuracy of UTC timestamps, a laptop PC was permanently synchronized by a Shelyak TimeBox in computer mode. The screen of a SEXTA device was recorded using a Basler 640-100 gm camera for 2 min at different acquisition frequencies. Three different acquisition software were used: Airylab Genika, SharpCap and PRISM as described in Materials and Methods. Figures 4A-4D show the delay between each frame timestamp subtracted from the SEXTA optical timestamp at each acquisition frequency. As shown in Figure 4A, the accuracy of the UTC timestamping done with Airylab's Genika is better than 1 ms (0.1 ms) UTC with a standard deviation of  $\pm 0.7$  ms and a constant time offset of +6 ms. These measures are similar to those presented in Figure 3, the variation of the standard deviation is possibly due to the use of different PCs for each measure (see Materials and Methods). As shown in Figures 4B and 4D, the variance of the UTC timestamps when using SharpCap as acquisition software was comparable to that observed when using Airylab Genika (standard deviation, Figures 4A, 4B and 4D). On the other hand, the analysis of the mean UTC delay when using SharpCap showed that the timestamp of the frames is recorded at the end of the exposure. When using SharpCap as acquisition software, the resulting timestamps add the exposure time of the frame to the constant time offset measured at +5 ms (Figures 4B and 4D).

In contrast, the variance of the UTC timestamps when using *PRISM* was greatly increased compared to the variance observed when using either *AiryLab Genika* or *SharpCap* (Figures 4C, 4D and 4E). Indeed, the standard deviation of the UTC timestamp delay was more than x140 (STD =  $\pm 139$  ms) times higher than those measured with *AiryLab Genika* and *SharpCap* (STD =  $\pm 0.7$  and  $\pm 1$  ms, respectively). The analysis of the mean UTC delay when using *PRISM* showed that the timestamp of the frames is done at the end of the exposure, but in contrast to either *AiryLab Genika* or *SharpCap* the time offset was not constant for each acquisition frequency. For this reason, a mean time offset of +37 ms was calculated from all different acquisition frequencies and used to correct the mean UTC time delays (Offset, Figure 4D). Moreover, the mean UTC delay was x77 times higher when using *PRISM* (mean delay = 7.7 ms) compared to those obtained with either *AiryLab Genika* or *SharpCap* (mean delay = 0.1 and 0.2 ms respectively). The difference in the mean and variance of the timestamps obtained with *PRISM* was compared to those obtained when using *AiryLab Genika* and *SharpCap* and found to be statistically different (Figure 4E and *Materials and Methods*).

In order to measure the UTC timestamp accuracy of frames recorded when using a camera triggered by a Shelyak TimeBox, a Basler 640-100gm GigE digital camera was used to record the screen of a SEXTA device at 1, 2, 4, 8, 10, 15, 20 and 24 FPS for two min. The recordings were done using *AiryLab Genika* as acquisition software, the frames were set to be triggered using the built-in external trigger of the camera as described in *Materials and Methods*. The results of the measures at different acquisition rates are shown in Figure 5. The delay between each frame timestamp was subtracted from the SEXTA optical timestamp; representative results for an acquisition frequency of 8 FPS are shown in Figure 5A and 5B. In Figure 5B at 8 FPS, we observed that the mean timestamp delay for all individual UTC-synchronized TTLs within a second was constant and measured to be better than 1 ms (0.9 ms) with a standard deviation of  $\pm 0.6$  ms (Figures 5B and 5C). No constant time offset was measured at any acquisition frequency as expected by the +16  $\mu$ s delay between the TTL and the start of the exposure announced by the manufacturer [28]. Figure 5C shows the delay between each frame timestamp subtracted from the SEXTA optical timestamp at each acquisition frequency. As shown

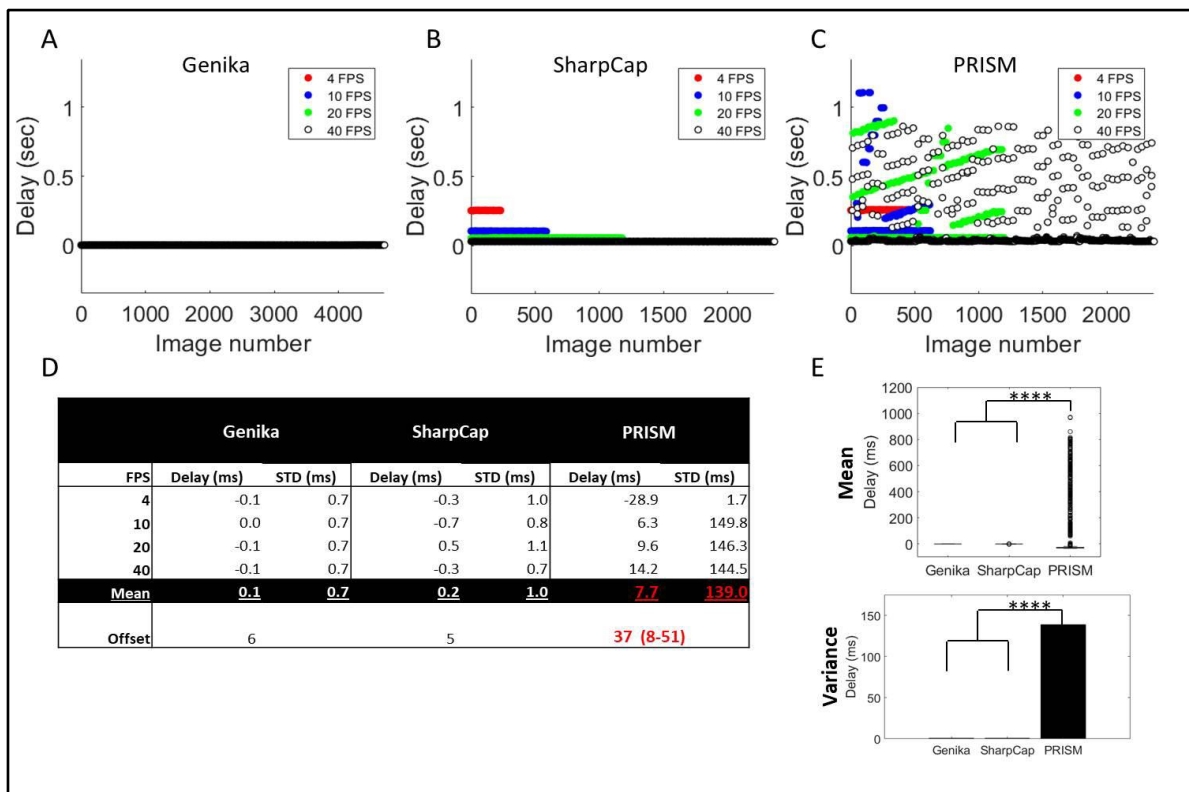


Figure 4A-E. The acquisition software is essential to allow the accurate timestamping of recordings. Different acquisition software were used to record a SEXTA device for 2 minutes at different frequencies with a Basler 640-100gm camera; the system's date/time was corrected using a Shelyak TimeBox in Computer mode. The results of the Delay (ms) between the frames timestamps and the SEXTA optical timestamps at different acquisition frequencies are displayed (4FPS filled red circles, 10 FPS filled blue circles, 20 FPS filled green circles and, 40 FPS empty black circles) for A - *AiryLab Genika*, B - *SharpCap* and C - *PRISM*. The results of the measures at different acquisition rates are shown in D, where the mean Delay (ms) for each acquisition was corrected for the constant time offset (milliseconds) of the recording and for the duration of the exposure in the case of *SharpCap* and *PRISM*. The mean delay and variance (standard deviation) for each frame recorded at all acquisition rates were calculated for each acquisition software and compared using a One-way ANOVA post-hoc test ( $p = 1.0698e-09$  \*\*\*\*) and are shown in E.

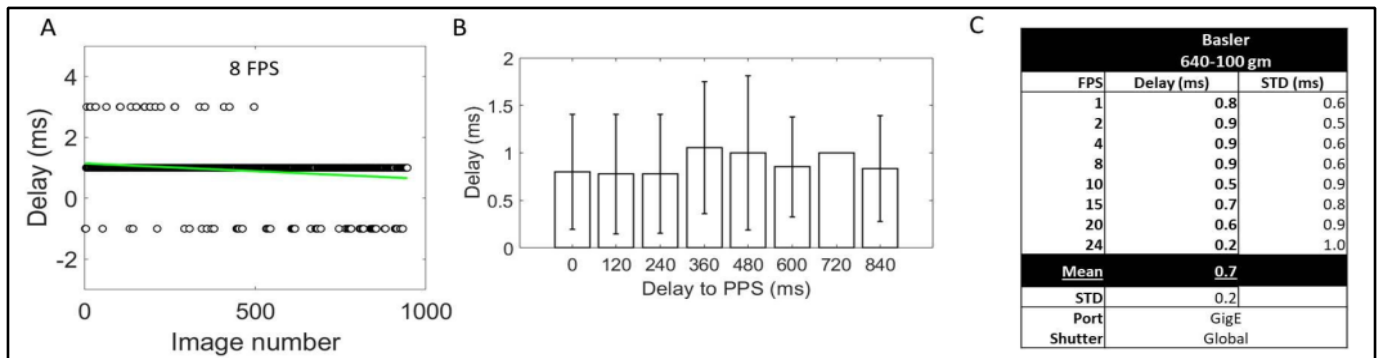


Figure 5A-C. Shelyak TimeBox in Trigger mode allows accurate millisecond timestamping of recordings with I/O triggered digital cameras. A I/O triggered Basler 640-100gm digital camera was used to record a SEXTA device for 2 minutes at different acquisition frequencies; the recording frames were triggered using a Shelyak TimeBox in Trigger mode at different frequencies. The recorded frames were captured using Airylab Genika as acquisition software.

A) Representative result of the Delay (ms) between the triggered frames timestamps and the SEXTA optical timestamps for the duration of the recording (8 FPS)

B) Delay of the individual triggered frames for each second during a representative recording (8 FPS).

The results of the measures at different acquisition rates are shown in C, where the mean Delay (ms) for each acquisition was measured.

in Figure 5C, the mean and standard variation of the UTC timestamping in trigger mode for all the recordings is less than 1 ms (0.7 ms) UTC and  $\pm 0.2$  ms respectively. These results show that the accuracy of the UTC timestamps recorded using the Shelyak TimeBox trigger mode is constant across the acquisition frequencies and to 1 ms UTC. It is important to remember that the configuration of the SEXTA used during these recordings offers a temporal resolution down to  $\pm 2$  ms referred to UTC [21].

During the last series of experiences, we wanted to measure the accuracy of the UTC synchronization of a PC permanently syn

chronized using a Shelyak TimeBox in computer mode for long periods of time. To achieve this, the OccuRec software [26] was installed and ran on a PC as described in Pavlov & Gault [13, 26]. OccuRec was used to record around 345.6 thousands (Figures 6A, 6D and 6G), 1.7 million (Figures 6B, 6E and 6H) and 518.4 thousands (Figures 6C, 6F and 6I) timestamps comparing the system date/time synchronized with a Shelyak TimeBox in computer mode compared to the IOTA-VTI for 4, 20 and 6 h respectively as described in Materials and Methods. As shown in Figures 6A and 6D when using the "Time correction" parameter "Slow", the PC date/time synchronization was regular over the 4 h with a mean

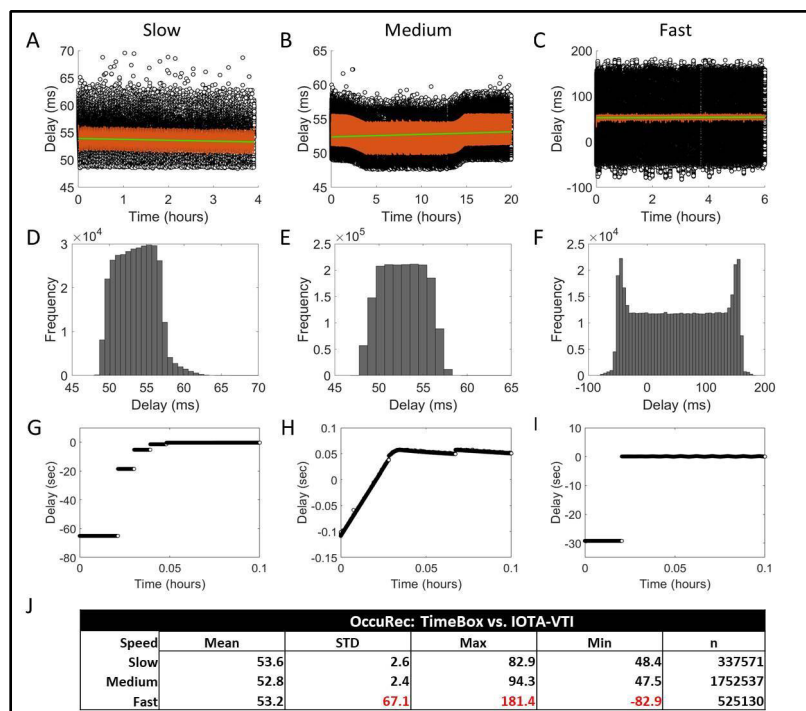


Figure 6A-I. Shelyak TimeBox in Computer mode allows stable and accurate timestamping of the system time/date over long periods of time.

Around 345.6 thousands (A and D), 1.7 million (B and E) and 518.4 thousands (C and F) Delay (ms) comparing the system date/time synchronized with a Shelyak TimeBox in Computer mode compared to the IOTA-VTI OCR timestamp were recorded for 4, 20 and 6 h (24 timestamps/second) using OccuRec.

Figures A and D correspond to the default Shelyak TimeBox time correction setting "Slow", Figures B and E corresponds to "Medium" and Figures C and F to "Fast".

The orange plot on Figures A, B and C represents a one-minute moving average of the Delay (ms), while the linear fit for each measure is shown in green. Histograms representing the Delay (ms) for each correction setting (Slow, Medium and Fast) are displayed in Figures D, E and F.

Figures G, H and I correspond to a magnification of the first 6 minutes preceding the recordings shown on Figures A, B and C respectively.

The results of the linear fits and statistical measures for each Shelyak TimeBox time correction setting are shown in J.

delay of 53.6 ms and a standard deviation of  $\pm 2.6$  ms (Figure 6J). Similarly, on Figures 6B and 6E when using the “Time correction” parameter “Medium”, the PC date/time synchronization was regular over the 20 hours with a mean delay of 52.8 ms and a standard deviation of  $\pm 2.4$  ms (Figure 6J). On the other hand, PC date/time synchronization was irregular when using the “Time correction” setting “Fast” on this system. The PC date/time synchronization using the “Time correction: Fast” showed high variations around the mean delay measured at 53.24 ms, and reflected in the dispersion of the individual measures around  $\pm 180$  ms, with a standard deviation of  $\pm 67.1$  ms as shown in the plot containing the individual measures (Figure 6C), the histogram representing frequency of the measures (Figure 6F) and the standard deviation around the mean (Figure 6J). It is important to note that these high variations in the PC system date/time synchronization were measured and accounted for in the Shelyak TimeBox log files produced during the synchronization routine. As described in Pavlov & Gault [Acquisition Delay, 13], the constant time delay of around 53 ms UTC is due to the time added by the frame grabber to digitise the recording coming from the IOTAVTI. These results show that it is important to measure the optimal correction rate of the synchronization for each system to avoid overcorrection and instability on the synchronization of the PC date/time when using the Shelyak TimeBox in computer mode.

Figure 6G, 6H and 6I correspond to a magnification of the first 6 min preceding the recordings shown on Figure 6A “Slow”, 6B “Medium” and 6C “Fast” respectively. The initial delay in the PC date/time was 1 min, 100 ms and 30 s for the three recordings respectively. We observed that in these three different settings, the Shelyak TimeBox was able to quickly and accurately correct the PC date/time under 3 min after the start of the synchronization (Figures 6G, 6H and 6I). These initial delays were accounted for by the Shelyak TimeBox from the first second of the synchronization and recorded in the log files produced during the recordings. As recommended in the Shelyak TimeBox user manual, accurate reading of the PC time in *Windows* environments needs to filter out random variations, extract a stable and accurate time base and correctly correct the system’s date/time [25]. For this reason, it is recommended to leave at least 15 min after the start of the PC date/time synchronization before recording astronomical phenomena, in order to obtain an accurate UTC and stable PC date/time. The results of the statistical measures on all three conditions are shown in Figure 6J.

## Discussion

As discussed in the introduction, the goal of this article was to measure the accuracy of the system date/time reading using different *Windows* functions, to independently test the Shelyak TimeBox using described methods [13, 21] for both computer and trigger modes, to assess the accuracy of the timestamping when using different cameras and acquisition software, and to measure the accuracy of the PC date/time synchronization at long periods of time.

We confirmed that the *Windows 10* `GetSystemTimePreciseAsFileTime` function outperforms the former *Windows 7* and earlier `GetSystemTime` function for accurately reading the system date/time (Figure 2). As noted in Pavlov & Gault [13, 15], *Windows 10* added additional improvements to its kernel and task scheduler that directly increases the accuracy of the system date/time. Also the `GetSystemTimePreciseAsFileTime` function resolution was increased up to the microsecond when compared to the millisecond only resolution of the `GetSystemTime` when reading the system date/time [27, 28]. For these reasons we recommend using *Windows 10* and reading the system date/time with the `GetSystemTimePreciseAsFileTime` function when recording astronomical occultations and other phenomena that need accurate UTC timestamping. The measures performed in this article were done in three different *Windows 10* PCs, probably with different *Windows 10* updated versions without altering the results. A number of users around the world routinely use the Shelyak TimeBox with their *Windows 10* PCs. So far, no complaints or problems due to *Windows 10* updates were raised for using the Shelyak TimeBox in different systems.

Moreover, the results shown in Figure 3 revealed that it is possible to accurately timestamp astronomical occultations up to 1-2 ms UTC when recorded using a PC permanently synchronized using a Shelyak TimeBox in computer mode. The results were similar when using Global/Rolling shutter and GigE/USB3 cameras; it is important to note that the recording made with a Rolling Shutter camera needs to be corrected for the line where the object appears as the timestamp corresponds to the time when the camera records the first line (see *Materials and Methods*). It would be interesting to consider adding an automatic correction of the timestamp for each object when recordings are done with Rolling Shutter cameras either in the acquisition software (*AiryLab Genika* or *SharpCap*) or in the reduction software like *Tangra* [30]. Also, the analysis of the mean delay for each camera and acquisition frequencies showed that there is a constant time offset for all acquisition frequencies for each recording camera (Figure 3D, Offset). This is one important element to consider to allow an accurate UTC timestamping when using digital systems; the Shelyak TimeBox possesses a built-in LED and a procedure that allows to measure this offset and a procedure is described on page 17 of the Shelyak TimeBox user manual [25].

The accuracy of the UTC timestamps obtained using the Shelyak TimeBox in computer mode was assessed in the past using different methods than those presented in this article [19, 20]. One of these measures consisted in recording a firing 1PPS LED and comparing the digital timestamps of the frames to the 1PPS LED optical timestamps as described in the Shelyak TimeBox user manual page 17 [25]. These measures were done using a Basler 1300-60gm GigE Global Shutter and a Raptor Photonics EMCCD Kite Global Shutter recording cameras with similar results that those presented in this article [20]. No apparent restrictions were observed for using digital cameras currently available for astronomical applications. Nonetheless, no measure was done to

assess the accuracy of the timestamping with neither DSLR nor mechanical shutter equipped cameras as we considered the evaluation of these devices out of the scope of this article.

As described in Barry et al. [21] camera control and acquisition software produces timestamps with widely varying fidelities to UTC. This was confirmed in Figure 4, where the recordings done with *PRISM* showed an extremely high timestamp variance, a non-constant time offset resulting in an inaccurate recording unsuitable for astronomical occultations. On the other hand, *AiryLab Genika* and *SharpCap* were able to record accurate UTC timestamps with low variance and a constant time offset. It is very important to note that *SharpCap* timestamps were done at the end of the exposure, adding this exposure time to the timestamp. This *SharpCap* characteristic was not described in the software documentation available at the date of the recordings, it would be preferable to explicitly describe this behaviour or to add a functionality allowing the date the timestamps at the start of the exposure by automatically subtracting the exposure time for each frame during the recording. As pointed out in this article, a vital factor in the accuracy of the timestamping is the choice of the recording software. Approved and tested recording software are able to accurately capture and timestamp frames, a variety of file formats can be used for the recordings if they are non-compressed and accurately timestamped.

Also, the UTC timestamp accuracy of frames recorded when using a camera triggered by a Shelyak TimeBox was measured and shown in Figure 5. These results showed that the accuracy of the UTC timestamps recorded using the Shelyak TimeBox trigger mode is better than 1 ms UTC and without any constant time offset. It is important to remember that the configuration of the SEXTA used during these recordings offers a temporal resolution down to  $\pm 2$  ms referred to UTC [21], so it will be interesting to test this mode using a higher resolution optical system like the EXposure Time Analyzer (EXTA) [30] or comparing the delay between the UTC-synchronized TTLs against TTL pulses produced by the UTC OP SYRTE atomic clock [18].

Furthermore, the results of the recordings shown in Figure 6 revealed that the Shelyak TimeBox was able to quickly and accurately correct the PC date/time under three minutes after the start of the synchronization (Figures 6G, 6H and 6I) and for long periods of time that exceed the 24-hours duration of the longest test. It is important to note that between the different parameters that played a role in the PC date/time for longer periods of time, the "time correction" setting showed to be important for having an optimal correction rate, avoid overcorrection and instability on the synchronization of the PC date/time when using the Shelyak TimeBox in computer mode.

A very broad range of USB and serial port GPS devices are available in the market. From simple navigation aids with no claim by the manufacturer of any time-keeping ability, to specialized devices where the manufacturer claims some degree of time accuracy achieved by various means. Apart from the Shelyak TimeBox no other device was tested in this article, authors cannot comment further on the accuracy of the timestamps obtained using these devices. The authors encourage the community of astronomers to test the timestamping accuracy of pertinent USB and serial port GPS devices in the future.

The results of the tests and recording presented in this article showed that the Shelyak TimeBox was able to allow quick and accurate UTC timestamped recordings using digital cameras. Using the Shelyak TimeBox in computer mode was measured to be accurate up to 1-2 ms UTC when using both GigE and USB3 cameras. It is important to note that in order to assure accuracy using the Shelyak TimeBox in computer mode, it is vital to choose an approved and tested software like *AiryLab Genika* and to measure and correct the constant time offset in each PC +camera system. An undergoing initiative by the IOTA timing commission works on testing and classing the most currently used acquisition software in astronomy on their ability to ensure accurate UTC timestamps during the recordings with digital cameras. Also, the results of the tests of the Shelyak TimeBox in trigger mode showed that its accuracy was beneath 1 ms UTC and without any constant

Shelyak Timbox Mode	Camera	Acquisition Software	Accuracy and STD	Notes
Computer	Basler 640-100gm, GigE and Global shutter	AiryLab Genika	$-0.1 \pm 0.1$ ms	Constant time offset +6 ms
Computer	ZWO ASI183MM-Pro, USB3 and Rolling shutter	AiryLab Genika	$-0.4 \pm 0.5$ ms	Constant time offset +16 ms. Rolling shutter correction <sup>*1</sup>
Computer	Basler acA3088-57um, USB3 and Rolling shutter	AiryLab Genika	$0.2 \pm 0.1$ ms	Constant time offset +8 ms. Rolling shutter correction <sup>*1</sup>
Trigger	Basler 640-100gm, GigE and Global shutter	AiryLab Genika	$0.9 \pm 0.6$ ms	No constant time offset
Computer	Basler 640-100gm, GigE and Global shutter	SharpCap	$0.2 \pm 1.0$ ms	Constant time offset +5 ms. Timestamp at the end of the exposure <sup>*2</sup>
Computer	Basler 640-100gm, GigE and Global shutter	PRISM	$7.7 \pm 139.0$ ms	Variant time offset. Timestamp at the end of the exposure <sup>*2</sup> . Not suited for timestamping
Computer	-	OccuRec	$53 \pm 2$ ms	Frame grabber offset of 53 ms <sup>*3</sup>

Figure 7. Summary table of the results. A table with the summary of the results is presented with the Shelyak TimeBox mode used (computer or trigger), the camera, acquisition software (*AiryLab Genika*, *SharpCap* or *PRISM*), the overall accuracy and standard deviation of the recordings and notes. <sup>\*1</sup> Rolling shutter cameras induce a drift of the exposure start/end through the array. A correction was applied (Materials and Methods). <sup>\*2</sup> The frames were timestamped at the end of the exposure. <sup>\*3</sup> Constant time delay 53 ms due to the time to digitize the recording coming from the IOTA-VTI with the frame grabber [13].

time offset. The accuracy in trigger mode could allow to increase the resolution of asteroids shape when recording occultations of brighter targets with large telescopes and sensitive cameras at higher acquisition frequency than those currently used.

In Figure 7, a table with the summary of the results is presented with the Shelyak TimeBox mode used (computer or trigger), the camera, acquisition software (*AiryLab Genika*, *SharpCap* or *PRISM*) and overall accuracy. The methodology used in this article for assessing the accuracy of the Shelyak TimeBox and the timestamping of different acquisition software/cameras can be used to test additional configurations used for occultations and other astronomical phenomena requiring precise UTC timestamping. It is interesting to note that being able to separate the UTC timestamping device from the recording camera will allow the use of last-generation, sensitive and low noise CCD, EMCCD and CMOS image sensors to be used for occultations. Also, the multimode design of the Shelyak TimeBox will allow amateur astronomers to use their current recording system without investing nor modifying their current hardware acquisition setup in most of the cases.

## References

- [1] McCarthy, D. D., Seidelmann, K. P. *Time: From Earth Rotation to Atomic Physics*. ISBN: 978-3-527-62795-0. (2009)
- [2] Trahan, R., Hyland, D. Phase retrieval applied to stellar occultation for asteroid silhouette characterization. *Appl Opt.* 2014 Jun 1;53(16): 3540-7.
- [3] The International Astronomical Union Minor Planet Center (MPC). <https://www.minorplanetcenter.net/iau/mpc.html>
- [4] Assafin, M., Camargo, J. I. B., Vieira Martins, R., Braga-Ribas, F., Sicardy, B., Andrei, A. H., Da Silva Neto, D. N. Candidate stellar occultations by large trans-Neptunian objects up to 2015. *Astronomy and Astrophysics*, volume 541, number A142. (2012)
- [5] Dias-Oliveira, A., Sicardy, B., Lellouch, E., Vieira-Martins, R., Assafin, M. et al. Pluto's atmosphere from stellar occultations in 2012 and 2013. *The Astrophysical Journal*. 811. 10.1088/0004-637X/811/1/53. (2015)
- [6] Braga-Ribas, F., Sicardy, B., Ortiz, J.L., Snodgrass, C., Roques, F. et al. A ring system detected around the Centaur (10199) Chariklo. *Nature*. 2014;508(7494):72-75. (2014)
- [7] IOTA-VTI v3, International Occultation Timing Association. <http://videotimers.com/home.html>
- [8] Midavaine Th. Imagerie à bas niveau de lumière – Fondamentaux et perspectives, Dossier Techniques de l'Ingénieur. E6570 11/02/2012.
- [9] QHY174M-GPS, Cooled USB 3.0 Planetary and Deep Sky COLDMOS Camera. <https://www.qhyccd.com/index.php?m=content&c=index&a=show&catid=94&id=46&cut=1>
- [10] Barry, M., Gault, D., Pavlov, H., Hanna, W., McEwan, A., & Filipović, M. A Digital Video System for Observing and Recording Occultations. *Publications of the Astronomical Society of Australia*, 32, E031. (2015)
- [11] Beisker, W. A Fast Digital CCD Camera with Precise Time Stamping for Use in Occultation Astronomy and Photometry, EPSC-DPS Joint Meeting 2019, held 2019 Sep 15-20 in Geneva, Switzerland.
- [12] Schweizer, A., Meister, S. DVTI, ESOP-38 Paris. <https://lesia.obspm.fr/lucky-star/esop38/doc/C1-3-A.Schweizer-S.Meister.pdf>
- [13] Pavlov, H., Gault, D. Using the Windows Clock with Network Time Protocol (NTP) for Occultation Timing. *Journal for Occultation Astronomy*, Volume 10 · No. 2 · 2020-2. [http://www.iota-es.de/JOA/JOA2020\\_2.pdf](http://www.iota-es.de/JOA/JOA2020_2.pdf)
- [14] Meinberg NTP software. <https://www.meinbergglobal.com/english/sw/ntp.htm>
- [15] Intel Software Developer Manual, section 17, page 17-42. <https://software.intel.com/sites/default/files/managed/a4/60/325384-sdm-vol-3abcd.pdf>
- [16] One Windows Kernel. <https://techcommunity.microsoft.com/t5/Windows-Kernel-Internals/One-Windows-Kernel/ba-p/267142>
- [17] Shelyak TimeBox Product page. <https://www.shelyak.com/produit/pf0063-timebox/?lang=en>
- [18] SYRTE - Systèmes de Référence Temps-Espace. <https://syрте.obspm.fr/spip/?lang=fr>
- [19] Leiva; R. A. Stellar occultations by Trans-Neptunian Objects and Centaurs: Application to Chariklo and its ring system. Doctoral dissertation, Université Pierre et Marie Curie - Paris VI, France. (2017) <https://tel.archives-ouvertes.fr/tel-01719296/document>
- [20] The TimeBox website <http://www.timeboxutc.com>
- [21] Barry, M., Gault, D., Bolt, G., McEwan, A., Filipović, M., & White, G. Verifying Timestamps of Occultation Observation Systems. *Publications of the Astronomical Society of Australia*, 32, E014. (2015)
- [22] AiryLab Genika Astro x64 product page and user manual. <https://airylab.com/genika-astro/>
- [23] Glover, R. SharpCap: image capture application designed primarily for Astrophotography and Video Astronomy. <https://www.sharpcap.co.uk/>
- [24] PRISM by ALCOR SYSTEM. <http://www.prism-astro.com/fr/index.html>
- [25] Shelyak TimeBox User Manual Rev A. [https://www.shelyak.com/wp-content/uploads/DC0035A-User\\_Manual\\_TimeBox\\_by\\_Shelyak.pdf](https://www.shelyak.com/wp-content/uploads/DC0035A-User_Manual_TimeBox_by_Shelyak.pdf)
- [26] Pavlov, H. OccuRec. Open source project. <http://www.hristopavlov.net/OccuRec/OccuRec.html>
- [27] GetSystemTimePreciseAsFileTime. <https://docs.microsoft.com/en-us/windows/win32/api/sysinfoapi/nf-sysinfoapi-getsystemtimepreciseasfiletime> Microsecond Resolution Time Services for Windows. <http://www.windowstimestamp.com/description>
- [28] Basler ace GigE - Product Documentation. <https://www.baslerweb.com/en/sales-support/downloads/document-downloads/basler-ace-gige-users-manual/>
- [29] Pavlov, H. *Tangra*: Software for video photometry and astrometry. <http://ascl.net/2004.002>
- [30] Dangl, G. EXposure Time Analyzer - EXTA. [http://www.dangl.at/exta/exta\\_e.htm](http://www.dangl.at/exta/exta_e.htm)

# Beyond Jupiter

## The World of Distant Minor Planets

Since the downgrading of Pluto in 2006 by the IAU, the planet Neptune marks the end of the zone of planets. Beyond Neptune, the world of icy large and small bodies, with and without an atmosphere (called Trans Neptunian Objects or TNOs) starts. This zone between Jupiter and Neptune is also host to mysterious objects, namely the Centaurs and the Neptune Trojans. All of these groups are summarized as "distant minor planets". Occultation observers investigate these members of our solar system, without ever using a spacecraft. The sheer number of these minor planets is huge. As of 2020 Dec 14, the *Minor Planet Center* listed 1182 Centaurs and 2542 TNOs.

In the coming years, JOA wants to portray a member of this world in every issue; needless to say not all of them will get an article here. The table shows you where to find the objects presented in former JOA issues. (KG)

No.	Name	Author	Link to Issue
944	Hidalgo	Oliver Klös	JOA 1 2019
2060	Chiron	Mike Kretlow	JOA 2 2020
5145	Pholus	Konrad Guhl	JOA 2 2016
8405	Asbolus	Oliver Klös	JOA 3 2016
10199	Chariklo	Mike Kretlow	JOA 1 2017
15760	Albion	Nikolai Wünsche	JOA 4 2019
20000	Varuna	Andre Knöfel	JOA 2 2017
28728	Ixion	Nikolai Wünsche	JOA 2 2018
47171	Lempo	Oliver Klös	JOA 4 2020
50000	Quaoar	Mike Kretlow	JOA 1 2020
54598	Bienor	Konrad Guhl	JOA 3 2018
60558	Echeclus	Oliver Klös	JOA 4 2017
90377	Sedna	Mike Kretlow	JOA 3 2020
90482	Orcus	Konrad Guhl	JOA 3 2017

### In this Issue:

(55576) Amycus

Konrad Guhl · IOTA/ES ·  
Berlin · Germany · kguhl@astw.de

**ABSTRACT:** Centaur object (55576) Amycus was first discovered in 2002 orbiting the Sun every 126.5 years. Its orbit takes it from well inside the path of Uranus at perihelion to outside that of Neptune whilst locked in a 3:4 resonance with Uranus. The diameter is close to 100 km. A photometric lightcurve indicates a rotation period of ~9.76 hours, although this value is rather approximate. Currently, no moons have been detected. This article highlights the need for observations of Amycus using the stellar occultation method in that the object has yet to be observed by this technique. The outlook for forthcoming occultations during 2021 is presented.

No.	Name	Author	Link to Issue
120347	Salacia	Andrea Guhl	JOA 4 2016
134340	Pluto	Andre Knöfel	JOA 2 2019
136108	Haumea	Mike Kretlow	JOA 3-2019
136199	Eris	Andre Knöfel	JOA 1 2018
136472	Makemake	Christoph Bittner	JOA 4 2018

## The Discovery

The object was discovered 2002 April 08 by the NEAT (Near-Earth Asteroid Tracking) at Palomar by the team, E. F. Helin, S. Pravdo, K. Lawrence, M. Hicks and R. Thicksten using the 1.2-m Schmidt + CCD (pictures of dome and telescope are given at JOA 3-2020, page 23). The object received the provisional designation 2002 GB<sub>10</sub> [1]. Pre-discovery images were found dating back to 1987 as listed on the JPL Small-Body Database.

## The Name

The object was identified as member of the family of small solar system bodies called Centaurs, the orbits of which are mostly confined between those of Jupiter and Neptune. Due to giant planets' perturbations, these objects have transient orbits with typical lifetimes of a few million years. The name Amycus = Amykos (Greek "Άμυκος ,") is also one of the Centaurs mentioned by the Greek poet, Ovid in his epic work entitled, *The Metamorphoses*. During the wedding party of Pirithoüs and Hippodameia, the centaurs attempted to carry off the bride and all female guests. This initiates a tough battle between the Lapiths and the Centaurs. In this battle, the centaur Amycus killed the lapith Keladon but was then slain by the lapith Pelates.

Unlike other centaurs, we have no visual representation of Amycus. Figure 1 shows a sarcophagus decoration from the first half of the 2nd century AD. This sarcophagus from Pianabella Necropolis is now at the Ostia Antica Museum and shows the Battle of the Centaurs, sometimes called the Centauromachy. Let us imagine that one of the centaurs shown is Amycus.

## The Orbit

The orbit (Figure 2) has an eccentricity of 0.394 and is inclined to the ecliptic by 13.3°. With a semi-major axis of 25.2 au, the distance from the sun varies between 15.2 au and 35.1 au.

Thus the orbit of Amycus leads from the perihelion inside the orbit of Uranus to an aphelion outside Neptune's orbit. Amycus is a Centaur according to the strict definition as an object with an orbit lying between Jupiter and Neptune ( $5.5 \text{ au} < a < 30.1 \text{ au}$ ) [2], but not quite distant enough to be called a TNO or Scattered Disk Object (SDO).

It last passed perihelion in 2003 and at present is approaching a distance of 23 au from the Sun as it slowly recedes towards aphelion. With an orbital period of 126.5 years, Amycus has a 3:4 resonance with Uranus [3].

## Physical Characteristics

Stansberry et al. published in [4] a diameter of  $76.3 \pm 12.5 \text{ km}$  calculated from observations by the *Spitzer Space Telescope* based on the Standard Thermal Model (STM). The observations were made at wavelengths near 24 and 70  $\mu\text{m}$ .

Bauer et. al. published in 2013 their analysis indicating a diameter of  $100.9 \pm 40.1 \text{ km}$ , based on *WISE* spacecraft flux measurements [5]. Perhaps the most accurate measurements were made using the *Herschel Space Telescope* [6]: these indicated a diameter of  $104 \pm 8 \text{ km}$ .

Measurements of the colour index show it to be a very red object [7] (Table 1).

Object	B-V	V-Rc	R-I
(5145) Pholus	$1.261 \pm 0.121$	$0.788 \pm 0.036$	$0.822 \pm 0.054$
(2060) Chiron	$0.700 \pm 0.020$	$0.361 \pm 0.017$	$0.325 \pm 0.023$
(55576) Amycus	$1.112 \pm 0.041$	$0.702 \pm 0.030$	$0.668 \pm 0.039$

Table 1. Colour index of Amycus lies between the reddest object of the class (Pholus) and the more blue object (Chiron).



Figure 1. Representation of the Battle of the Centaurs

Source: [https://en.wikipedia.org/wiki/File:Sarcophago\\_con\\_centaumachia,\\_II\\_secolo,\\_da\\_procoio\\_di\\_pianabella,\\_01.JPG](https://en.wikipedia.org/wiki/File:Sarcophago_con_centaumachia,_II_secolo,_da_procoio_di_pianabella,_01.JPG)

Repro: <https://commons.wikimedia.org/wiki/User:Sailko>

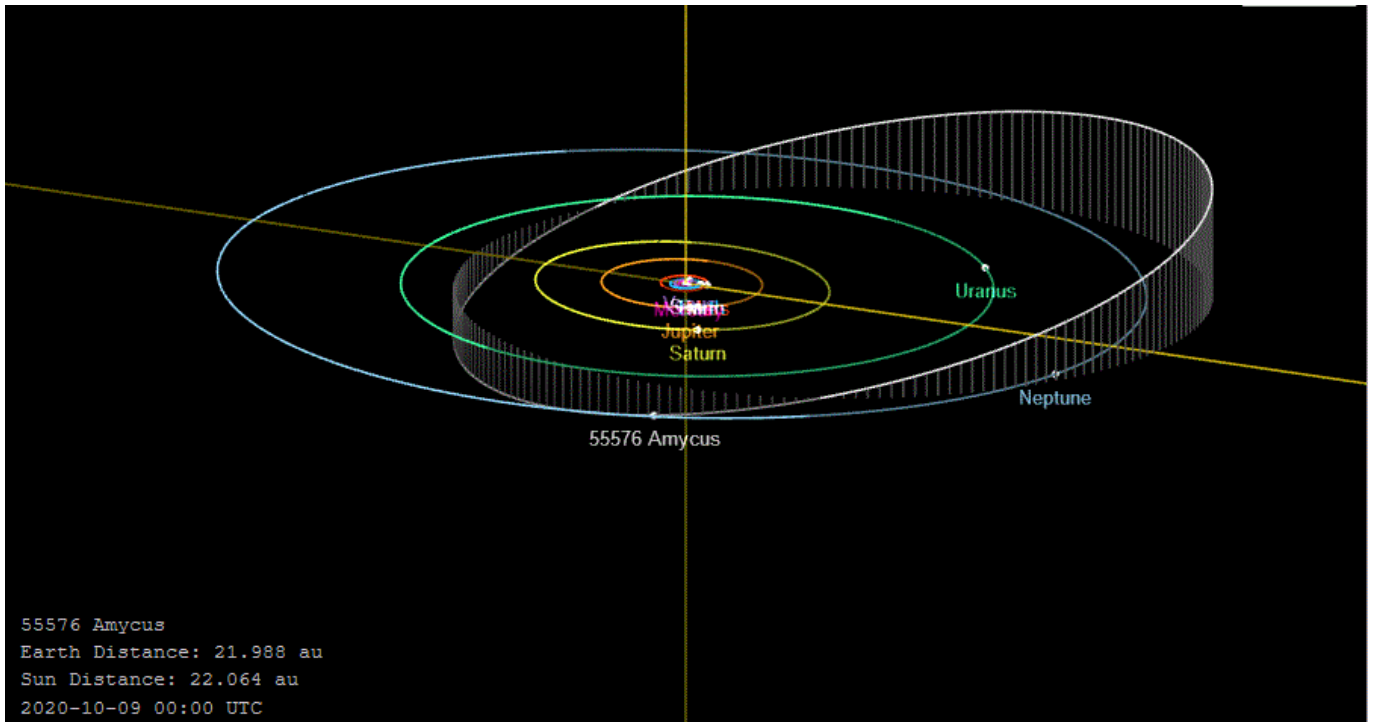


Figure 2. Orbit diagram and position for 2020. JPL Small-Body Database Browser, <https://ssd.jpl.nasa.gov/sbdb.cgi?sstr=55576>

The apparent brightness of Amycus at perihelion is 19.3V but has now faded to 20.6V - 20.9V as it moves further away from the Sun and Earth. The physical properties of Amycus are rather poorly known. The JPL database lists an absolute magnitude, H of 7.8. Other references show significant deviations from this value, notably 8.07 [4], 7.46 [5], 8.27 [6], 7.77 [7] and 7.12 [8]. Likewise the geometric albedo was thought to be quite high at 0.18 [4, 5] but the *Herschel* data has shown it to be more typical of centaur objects at  $0.083 \pm 0.016$  [6] but with a flux excess at  $24 \mu\text{m}$ , which

may be related to two different albedo terrains. In Ref. [9], the authors published lightcurve measurements compatible with a rotation period of 9.76 h. The amplitude of the observed light curve was 0.16 mag in 2003. The lightcurve published in this paper is shown in Figure 3.

Interesting to see that in [9] Amycus is called a TNO (see above). At this point, there have been no moons discovered orbiting Amycus.

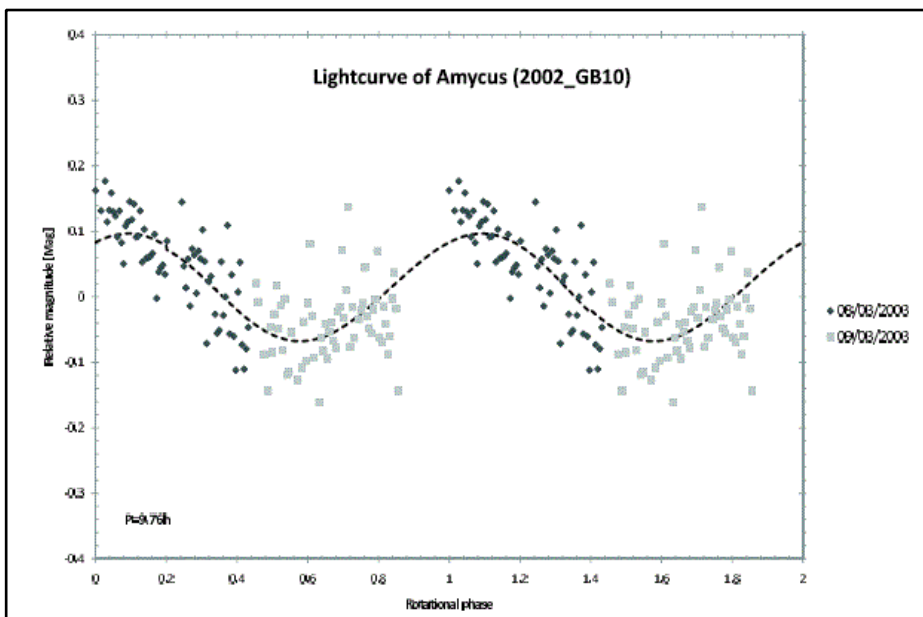


Figure 3. Lightcurve of Amycus, observation and Fourier Series fit [5].

## Occultations by Amycus

In the past, some occultations by Amycus were predicted and occultation observers across North America and Europe have attempted to observe them. Up to now, no positive observations have been reported. Josselin Desmars of Bruno Sicardy's Lucky Star Project (with help of the IAA-Granada team and the Rio team) calculated more possible stellar occultations by Amycus for 2021. The predictions sorted by date, and/or star magnitude and/or area can be found at <http://lesia.obspm.fr/lucky-star/predictions/>

For 2021, the team calculates 24 events for stars as faint as 18 mag potentially visible from Earth. With the current uncertainties, in 15 cases the shadow only passes close to the Earth. The brightest star in the list of candidates for which the shadow path crosses Earth is magnitude 13.4G. This event is calculated to be visible from parts of southern Africa and South America on 2021 Jul 30 (Figure 4).

The next brightest star predicted to be occulted during 2021 is magnitude 15.6G, the path of which may cross southern Europe (at a low altitude) and North Africa on 2021 Sep 13. Observations of this particular event are strongly encouraged (Figure 5).

## References

- [1] MPEC 2002-H11  
<https://minorplanetcenter.net/iau/mpec/K02/K02H11.html>
- [2] Centaur orbit classification  
[https://ssd.jpl.nasa.gov/sbdb\\_help.cgi?class=CEN](https://ssd.jpl.nasa.gov/sbdb_help.cgi?class=CEN)
- [3] J. Horner, N.W. Evans and M.E. Bailey: "Simulations of the Population of Centaurs I: The Bulk Statistics", *Monthly Notices of the Royal Astronomical Society*, 354 (3), 798–810, (2004)  
<https://arxiv.org/abs/astro-ph/0407400>
- [4] J. Stansberry et al., "Physical Properties of Kuiper Belt and Centaur Objects: Constraints from Spitzer Space Telescope", in "The Solar System Beyond Neptune" M. A. Barucci, H. Boehnhardt, D. P. Cruikshank, and A. Morbidelli (eds.), University of Arizona Press, Tucson, pp. 161-179 (2008)  
<https://arxiv.org/pdf/astro-ph/0702538.pdf>
- [5] J.M. Bauer et al., "CENTAURS AND SCATTERED DISK OBJECTS IN THE THERMAL INFRARED: ANALYSIS OF WISE/NEOWISE OBSERVATIONS". *The Astrophysical Journal*, 773, 22 (11pp), 2013 August 10  
<https://iopscience.iop.org/article/10.1088/0004-637X/773/1/22/pdf>
- [6] R. Duffard et al., "TNOs are cool!: A survey of the transneptunian region: A Herschel-PACS view of 16 Centaurs". *Astron. & Astrophys.*, 564: A92, (2013)  
<https://arxiv.org/abs/1309.0946>
- [7] O.R. Hainaut, H. Boehnhardt, and S. Protopapa, "Colours of minor bodies in the outer solar system". *Astron. & Astrophys.*, A115 (2012)  
[http://www.eso.org/~ohainaut/MBOSS/aa19566-12\\_tap.pdf](http://www.eso.org/~ohainaut/MBOSS/aa19566-12_tap.pdf)
- [8] Minor Planet & Comet Ephemeris Service, Minor Planet Center (accessed 2020 Oct 24)  
<https://minorplanetcenter.net/iau/MPEph/MPEph.html>

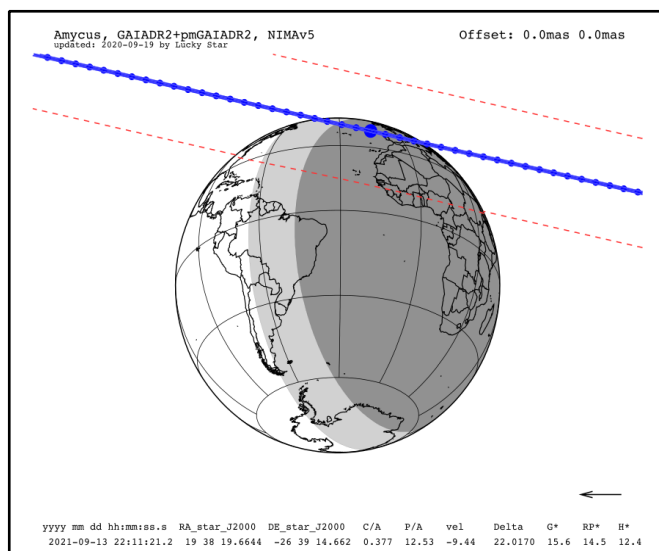
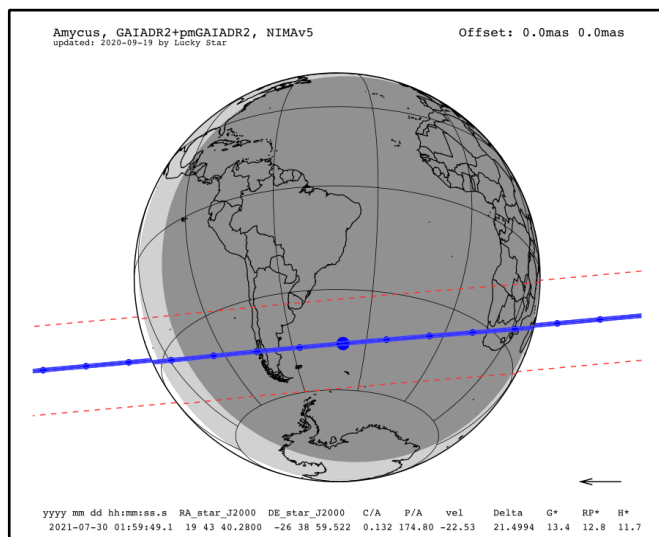


Figure 4 (top). Occultation of a 13.4 mag star by Amycus on 2021 July 30.

Figure 5 (bottom). Occultation of a 15.6 mag star by Amycus on 2021 September 13

Source: <http://lesia.obspm.fr/lucky-star/predictions/>

- [9] A. Thirouin et al.: "Short-term variability of a sample of 29 trans-Neptunian objects and Centaurs". *Astron. & Astrophys.*, 522, A93, (2010)  
<https://arxiv.org/pdf/1004.4841.pdf>

## Useful Links

Deep Ecliptic Survey, <https://web.archive.org/web/20040829233039/http://www.lowell.edu:80/Research/DES/index.html>

JPL Small-Body Database, <http://ssd.jpl.nasa.gov/sbdb.cgi>

Spacewatch homepage, <http://spacewatch.lpl.arizona.edu>

Minor Planet Center, <http://www.minorplanetcenter.net/>

# The International Occultation Timing Association's 38<sup>th</sup> Annual Meeting, 2020 July 25-26 via Zoom Online

Richard Nugent · IOTA · Dripping Springs, Texas · USA · RNugent@wt.net

**ABSTRACT:** IOTA's 2020 Annual Meeting was held via Zoom online on 2020 July 25-26. Numerous presentations were made by members of the IOTA community worldwide. Upwards of 83 attendees participated in the meeting via Zoom which is a record for IOTA meeting attendance.

The 38<sup>th</sup> annual meeting of the International Occultation Timing Association was held Saturday and Sunday July 25-26, 2020 via Zoom online. The meeting schedule and agenda are located on the IOTA web site presentation page [1].

Ted Blank has created a YouTube link and uploaded all the presentations [2].

The meeting started out with 68 participants and this number fluctuated to 78 attendees on Saturday and reached 83 participants on Sunday. *This is a record for attendance at any IOTA meeting!*

## Saturday 25<sup>th</sup> July 2020 - Day 1

IOTA's Vice President Dr. Roger Venable opened and welcomed everyone to the meeting. Ted Blank gave instructions for using Zoom functions for this year's fully online meeting.

### Business Meeting

Treasurer Joan Dunham presented IOTA's financials and membership status. In 2019 the *Journal for Occultation Astronomy (JOA)* expensive print memberships were ended since all of those subscribers were e-mail and internet users.

A summary of the year's income/expense report (September 2019 to July 2020):

Income:	
Membership.....	\$1,385.50
Royalties (VTI & RunCam sales) .....	\$6,000.00
Donation .....	\$162.96
<b>TOTAL INCOME .....</b>	<b>\$7,548.45</b>

Expenses:	
JOA Production .....	\$1514.46*
VTI Production .....	\$5,070.00
Awards .....	\$184.00
<b>TOTAL EXPENSES .....</b>	<b>\$6,584.46</b>

NET Income: \$964.00

\*Note: IOTA has not yet been billed for production expenses for *JOA 2020-3*.

### IOTA Balance Sheet

Cash on Hand - Bank and Paypal.....	\$12,154.87
MADAMO Award [3].....	\$3,000.00
Funds dedicated for asteroid moon discovery and confirmation.	
Reserve Fund - Web Server.....	\$500.00

### IOTA Membership and Subscription:

Membership only: 113
Library membership: 2
North American (USA and Canada) members: 99
Other (India, Australian, New Zealand, European): 6

Joan described IOTA's new affiliate membership which is a non-voting membership for organizations, schools, clubs, businesses but not for individuals. It allows widespread distribution of event information – such as bright stellar occultations by asteroids, bright grazing occultations, etc. This membership will be renewed annually and is free of charge.

### Awards

Executive Secretary Richard Nugent then presented the IOTA's *Homer F. Daboll*, *David E. Laird* and the *Lifetime achievement Awards*. The *Homer F. DaBoll Award* is given to recognize significant contributions to the field of occultation science and to the work of IOTA. This year's recipient is Tony Barry from New South Wales, Australia.

Tony's contributions to the field of occultation science are numerous and significant. He became involved in occultation observing in 2009 after attending a presentation by Dave Gault at the Western Sydney Amateur Astronomy Group. Tony soon became aware of the need to develop a low cost but accurate timing device for use during occultation observations. Seeing this need, Tony has developed two devices to ensure the time-stamp accuracy of occultation observations:

- IOTA-VTI - a Video Time Inserter that has time-stamps with GPS based UTC. To date, over 300 IOTA-VTI's have been sold.



Figure 1 - 3. The recipients of the IOTA awards 2020: Tony Barry - Homer F. DaBoll Award, Derald Nye - David Laird Award and Walt "Rob" Robinson - Lifetime Achievement Award (from left to right).

- SEXTA – Southern EXposure Timing Array is a GPS disciplined device and analysis App. designed to verify the time-stamps of any camera imaging system. The design of SEXTA is available Open Source – available to anyone who needs it, free of charge. Currently six SEXTAs have been constructed.

In addition to the IOTA-VTI and SEXTA, Tony has also been the lead or co-author on a number of published papers in the field of occultation science.

The *David E. Laird Award* is given to recognize those who, more than 15 years ago, made significant contributions to occultation science and to the work of the IOTA. This year's *David E. Laird Award* recipient is Derald Nye from Arizona. Derald is an avid observer, who has travelled worldwide for the most unusual occultations and eclipses. On 1989 November 22 using binoculars, Derald timed an occultation of a 7.1 mag. star by (15) Eunomia from the Amazon River, the only asteroidal occultation known to have been observed from a ship. On 1998 April 23, he and wife Denise observed the rare simultaneous lunar occultations of Venus and Jupiter from Ascension Island. On 2005 October 19, he timed an occultation of Regulus by (166) Rhodope from Portugal along with several other observers.

To date, he has seen 45 eclipses, and collected data on many of them for IOTA's long term solar radius study. Derald has also helped with the early promotion of grazes and has maintained the *Occultation Newsletter* archives since the 1980's.

Derald and his wife Denise also have the honour of having asteroid (3685) Derdenye named in their honour. It was discovered 1981 March 1 at Siding Spring Observatory, New South Wales.

The *IOTA Lifetime Achievement Award* is given, as needed, to recognize outstanding contributions to the science of occultations and to the work of the IOTA over an extended period of the recipient's lifetime and is conferred by the IOTA Board as needed. This year's *Lifetime Achievement Award*'s recipient is Walt 'Rob' Robinson. For several decades, Walt has provided occultation predictions for observers. He has maintained IOTA's lunar occultation website since 1995, observed over 1,000 occultations, recovering 100's of lost observations confirming grazes of unknown stars, and has distributed *Occult* software worldwide. In 2006, Walt coauthored the book with Hal Povenmire, "*Occultation Observer's Handbook*".

For information on IOTA's awards, including previous awardees, see the award webpage [4].

### Technical Sessions

Alex Knox presented a talk "*Automating Telescopes to Observe Occultation Events*". Her telescope system consisted of a Celestron NexStar5 with the StarSense AutoAlign feature, the RunCam Night Eagle 2 Pro camera recording on a Panasonic Toughbook computer through a USB port. The basic sequence is:

- IOTA's video capture software was used to record twice: first, as input for the plate solve software and second, at the time of the event
- *ImageJ*, an image processing software, was used to convert the first recording by the video capture software from its avi format to FITS format, which is accessible to the plate solving software.
- The plate solve was run on *AstroTortilla*, a software driven by the *Astrometry.net* plate solver engine

**Tony George** spoke on the chords of the (229) Adelinda event from 2020 Jun 17. Tony showed his jagged light curve he obtained which he first declared inconclusive. Using *PyOTE*, Phil Stuart reported a 0.33 mag drop event and his position was in line with Tony's observation. Wayne Thomas sent his video to Tony and using *PyMovie*, he found an event. Richard Nolthenius also observed this occultation at 64x integration but was unsure if he had an event. But he had a "blip" in the light curve that indicated an event. When plotted with the rest of the chords, his observation made a decent fit compared to the other observations.

**Tony George** then spoke about use of a digital noise reduction (DNR) with the Watec 910HX camera. His basic message was to never use the 3DNR noise reduction option in camera settings. Most chips inside our cameras pick up noise from the other electronic components within the camera. The 3DNR has the effect of applying a running average making occultation events appear gradual instead of instantaneous. He is of the opinion that the 3DNR should not be used. Tony mentioned that the Watec 910HX turns this feature on automatically when turned on, so be sure to turn it off on start up.

**Bob Anderson** talked about *PyMovie*. Bob created *PyMovie* to help with star images that were smeared either from wind shake and/or rising hot air heating effects. A computed mask would cover the smeared star image vs. the classic circular mask common to both *Limovie* and *Tangra*. Bob showed an example video using *PyMovie* and how it removed noise pixels to help identify stars as compared to a star chart. He recommended using a background aperture in the star field to calibrate/verify that the target star tracking aperture is working well.

Bob then discussed the issues of false positives and the normalization function when used with the target star and comparison star with *PyOTE*. Several questions came in after Bob's talk and he demonstrated the normalization function and other useful features of *PyOTE*.

**Suhas Gurjar** from IOTA's India Section presented a history of India's occultation history. The first asteroid event observed was (1243) Pamela occultation results from Feb 2013. In Dec 2016 Paul Maley helped organize 20 video stations for the (22) Kalliope event. 8 chords were obtained and the result is shown in Figure 4. With no internet information for India occultations events, on 2019 May 3, the India IOTA section was formed [5]. India has very few observers, and Suhas is working on expanding this. He has published articles in their local online newspapers advertising such events. He also has a Facebook page advertising India occultations.

**Paul Maley** then introduced **Atila Poro** from Iran, President of IOTA/ME (Middle East) section. He presented a history of the IOTA/ME section and some of the observations and methods they use. He talked about the work his members are doing now including studying the sizes of 3 asteroids, TNO's and other objects. Some occultation techniques are being introduced in schools.

**Dr. David Dunham** spoke on the best grazing occultations of the past year and best upcoming grazes 2020 and 2021. He started with the video of a spectacular graze of Aldebaran from 2017 March 5 in Canada. 5 observers made observations and a combined video of all the D's and R's was shown.

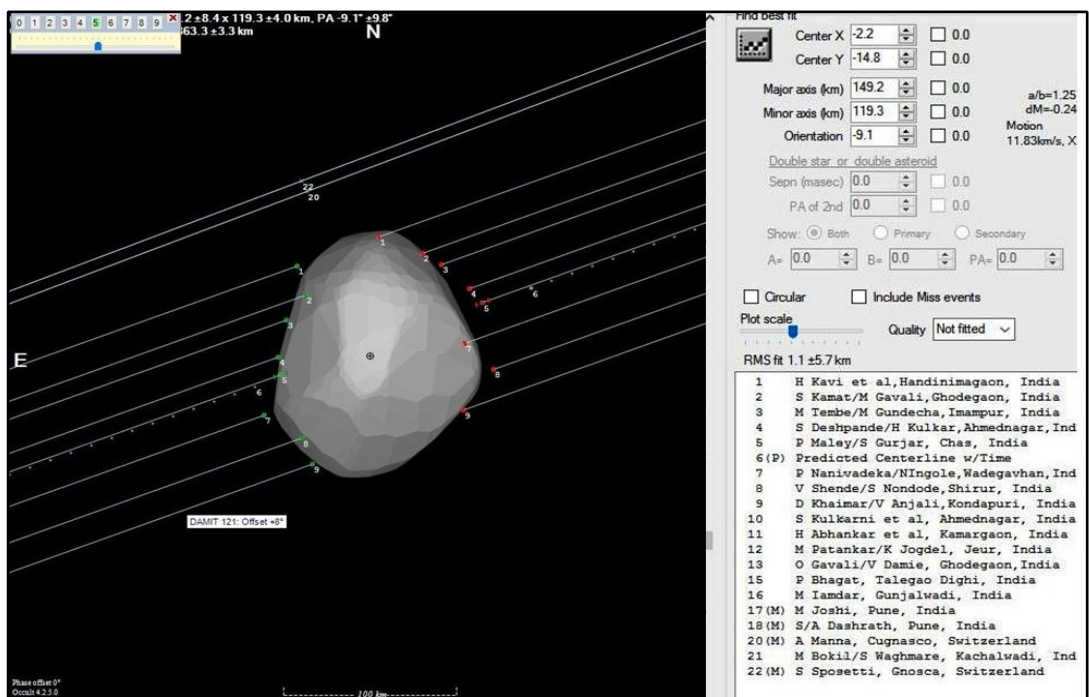


Figure 4. (22) Kalliope observed from India, 2016 Dec 24.

Additional events:

- 2019 May 11, ZC 1298, they observed over 40 occultations that night. Plus 5 D's and R's with the 6.5 mag star ZC 1298.
- 2020 Jan 2, 33 Piscium, 4.6 mag, path crossed Phoenix, Arizona area suburbs. They got 3 D's and 4 R's.
- 2020 Apr 28, Milky Way passage by the crescent Moon. From Fountain Hills, Arizona they observed some 26 occultations. Several stars were listed as double stars, but they didn't see evidence of this in their observations. For a few of the brighter events, Joan and David ran their QHY camera at higher frame rate than video rates, resolving the "toe" of the Fresnel diffraction pattern.

David then discussed future graze events for 2020 and 2021, Graze stars 5.0 mag or brighter are published in *JOA* and stars brighter than 7.5 mag in the *RASC Observer's Handbook*. The 2020 World Map for these grazes is available on [6].

IOTA's President **Steve Preston** spoke on the best asteroid occultations for the upcoming year for North America. With Gaia star position data there is a higher probability of accuracy of asteroid event predictions.

Best occultations in 2021, North America:

- Jan 19, (60558) Echeclus.  
Currently a large prediction error, Steve will update
- Mar 18, (8) Flora, target star: 7.2 mag
- Apr 2, Jupiter, 44 Cap, 5,8 mag, duration 72 minutes
- Jul 27, (6) Hebe, target star 8.2 mag
- Sep 7, (191) Kolga, target star 7.1 mag
- Sep 20, (762) Pulcova, target star 7.1 mag
- Oct 20, (3548) Eurybates, target star 12.1 mag.  
Call for observation by SwRI.

**John Moore** talked about the best observed North American asteroid occultations for the past year. He started with IOTA North American statistics 3-year summary. There is an increasing trend of observations in the past 3 years 2017 – 2020 (Table 1).

Year	Total observations	Positive chords	Negative chords
2017	132	232	79
2018	185	351	121
2019	206	372	178

Table 1. Trend of observations 2017 - 2020.

Busiest North American asteroid occultation observers in 2020 with number of chords are shown in Table 2.

Name	Chords #
David & Joan Dunham	67
Paul Maley	45
Roger Venable	33
Dave Oesper	26
Tony George	26
Steve Messner	25
John Moore	25
Wayne Thomas	23
Jerry Bardecker	18
Chris Anderson	17

Table 2. Busiest North American asteroid occultation observers in 2019.

2019's most interesting observations:

2019 Jul 29, (3200) Phaethon – a total of 52 chords, with 6 positives and 46 negatives. Chord coordination done by David Dunham. Phaethon is the target for the *JAXA Destiny* mission, launch date ~ 2022. Phaethon was captured again on 2019 Sep 29.

**Dave Herald** discussed the best non-North American asteroid occultations for the past year 2019. In 2019 worldwide asteroid occultation observations were over 500 and showing a growing trend the past few years. Compared to the 1990's the number of non-usable events has dropped significantly. This is because the 1990's had lots of visual observations, whence the past 10 years we now use video and GPS-based timing techniques.

He listed the number of worldwide asteroid observations vs. the average number of observations/event:

- 2017: 939 observations, 334 events, 2.8 obs/event
- 2018: 1490 observations, 504 events, 3.0 obs/event
- 2019: 1666 observations, 586 events, 2.8 obs/event

Dave then showed world stats of asteroid observations by region:

Region	2019	2018	2017
Australasia	132	142	68
Europe	171	148	95
Japan	56	34	22
US	287	183	130
South America	20	23	17
Other	22	15	-
Total	688	545	332

Table 3. Asteroid occultation observations by region 2017 - 2019.

He mentioned double stars discovered during occultations are usually found in the 1 to 100 mas (milliarcsecond) range separation. Compare this to Gaia's resolution of ~100 mas.

Dave then showed 11 of the best profiles for 2019 and compared occultation derived diameters vs. those of IR satellites (Table 4).

		Diameter (km)			
		Occultation	IR satellite		
Date	Asteroid	Fitted	Neowise	AcuA	IRAS
Jan 17	(984) Gretia	36	32 ± 3	-	-
Feb 10	(71) Niobe	84	80 ± 10	86 ± 6	83 ± 10
Feb 12	(334) Chicago	179	199 ± 25	180 ± 13	159 ± 25
Apr 22	(145) Adeona <sup>A</sup>	142	127 ± 13	144 ± 21	151 ± 18
Jul 29	(3200) Phaethon <sup>B</sup>	5.3	-	4.8 ± 1.0	5.1 ± 0.6
Aug 14	(163) Erigone	74	81 ± 11	74 ± 5	-
Aug 28	(624) Hektor	181	147 ± 17	147 ± 11	-
Oct 1	(247) Eukrate	308	305 ± 17	212 ± 14	-
Oct 15	(144) Vibia	144	155 ± 38	147 ± 11	142 ± 17
Oct 24	(16) Psyche	216	288 ± 33	227 ± 20	253 ± 29
Oct 29	(87) Sylvia	288	253 ± 28	262 ± 19	261 ± 29
	Romulus <sup>C</sup>	36 x 20			
	Remus <sup>D</sup>	13 x 9			

<sup>A</sup> Occultation of double star of 5.3 mas separation in PA 133°

<sup>B</sup> Dave Herald mentioned that gravitational deflection moved the actual location of the asteroid approximately 1 diameter compared to the 3 predictions made.

<sup>C</sup> Sep 0.513" in PA 75°

<sup>D</sup> Sep 0.265" in PA 91°

Table 4. Diameters of asteroid derived from occultations in 2019 vs. measurements of IR satellites.

Steve Kerr spoke about recent occultations happenings in Australia and New Zealand. Going back to 2008, he showed the trend of observed events. There were 47 successful chords in 2008 and over the years increased to 180 successful chords in 2019. He then showed profiles of some of the better observed asteroid events, (349) Dembowska on 2019 Jun 18, (18) Melpomene on 2019 Oct 4, (925) Alponsina on 2019 Oct 23, (458) Hercynia on 2019 Dec 17.

## Sunday 26<sup>th</sup> July 2020 - Day 2

Kai Getrost discussed calibration issues with the QHY174M-GPS. Calibration is important for timestamp accuracy, and exposure accuracy (which could be off by 100ms). Calibration is not a one time setting, when some camera settings are changed, the calibration must be updated. Kai demonstrated how using the built in LED with its pulses, he could calibrate to GPS time. He also discussed why calibration was needed more often due to occasional frozen time stamps and other issues. Kai recommended re-calibrating each time any combination of settings (such as exposure) are changed. He listed several references/resources on the QHY174M-GPS camera:

- SharpCap forums [7]
- Dr. Christian Weber's IOTA/ES Berlin workshop notes on the QHY174M-GPS [8].

Kai next discussed tips and tricks when using the QHY174M-GPS camera – General Issues, Advice and Best Practices. Kai mentioned that the typical 12v power connector inserted in a car accessory

adapter can cause problems: sometimes the tip comes up just short of connecting. His solution was to add a piece of solder to make it longer. He mentioned that more binning will not improve S/N ratios as it does with CCD cameras.

Kai offered a few good practice hardware issues: Always connect to 12v power. This runs the TEC and fan. One should always connect the camera at start of a session – this minimizes thermal shock for late camera power ups. A few other common sense things should be done also – secure all cables on scope with rubber bands/Velcro. And if it's cold outside, use a zip lock bag to prevent condensation.

Dr. Joan Dunham discussed using a 16" SkyWatcher telescope with the QHY174M-GPS camera. Joan talked about how they prepare to observe. First they collimate the telescope. They use a video finder aligned with the scope for later easy locating of target stars. A 2-star alignment is used for aligning the telescope. With the red sensitive chip of the RunCam camera, the FOV may not match the finder charts including the asteroid and target star – she advised to go ahead and get the data and reduce it later. Joan uses an observing table next to the telescope - its holds finder charts, batteries, computer, mouse, IOTA-VTI, flashlight, etc.

Since June of this year, Joan and David tried 4 asteroid events from the sidewalk near their house: (803) Picka 2020 June 3, 2013 LU28 (miss), (466) Tsiphone 2020 July 2 (failed) and (53) Kalypso 2020 July 2 (miss). They have even done lunar occultations from their bedroom window.

Joan's equipment wish list: Enhanced pre-point charts on a laptop with night mode lighting instead of paper charts, camera with IOTA-VTI GPS capabilities, onboard temporary capture to avoid dropped frames. Joan also mentioned that the USB 3.0 standard does not specify a maximum cord length but the maximum practical length for copper wiring to meet the electrical specs is 3 m (9.8 ft).

David Dunham then talked about the *Ode to V1943 Sagittarii* and how it foiled his station 3 observation of the (303) Josephina event on 2020 Jul 10. A few minutes before the occultation, the problem was that the pattern of stars in the FOV of his non-tracking 120mm "maxi" scope video didn't match the finder chart. The problem was solved 2 nights later. Turns out the red sensitive RunCam camera showed red stars not visible visually through his finder and this was confusing when the occultation time draws near. David showed a few slides with a method using *Guide 8/9* to identify these red stars by using *Guide's* option to show variable stars.

At the NASA *Small Bodies Assessment Group Conference* in January 2019, Marc Buie (SwRI) made a good case for officially supporting occultation work. Professional astronomers took notice with his talk and the publicity from SwRI's 2017 and 2018 Arrokoth (MU69) campaigns. Papers are due 2020 Aug 15 for the next Astronomical Decadal Survey for proposed missions and 2020 Sep 15 for others.

David Dunham next talked about the (3200) Phaethon occultation from 2019 Jul 29 visible over California, Nevada and Colorado. It's the target of the Japanese Space Agency's (JAXA) *Destiny* flyby in 2025, hence the need for occultation observations to provide an accurate position to refine it's orbit for the mission. Phaethon's small 5 km size made predictions a challenge. The plan was to have 66 stations spread out over a 45 km range. Not all stations could be filled, and 11 didn't get any data. Figure 5 shows the resulting occultation profile.

David then talked about the attempted 2019 Sep 29 occultation by Phaethon tried by 4 observers. The observations were too poor to improve on the size and shape of Phaethon but they did provide an astrometric point which matched the *JPL Horizons* Team solution 707 well. Two more events with Phaethon occurred on 2019 Oct 12 with an 11.3 mag star, and 2019 Oct 15 over Japan where only two stations got data, 8 other stations had clouds.

David then showed his typical paver stone mount setup for remote stations and how it can reach stars down to 13 mag. A major advantage of the paver stone mounts is that the stones are sturdy, cheap, and can be pre-pointed the night before, then the scope carefully removed and the paver stone can be left at the site.

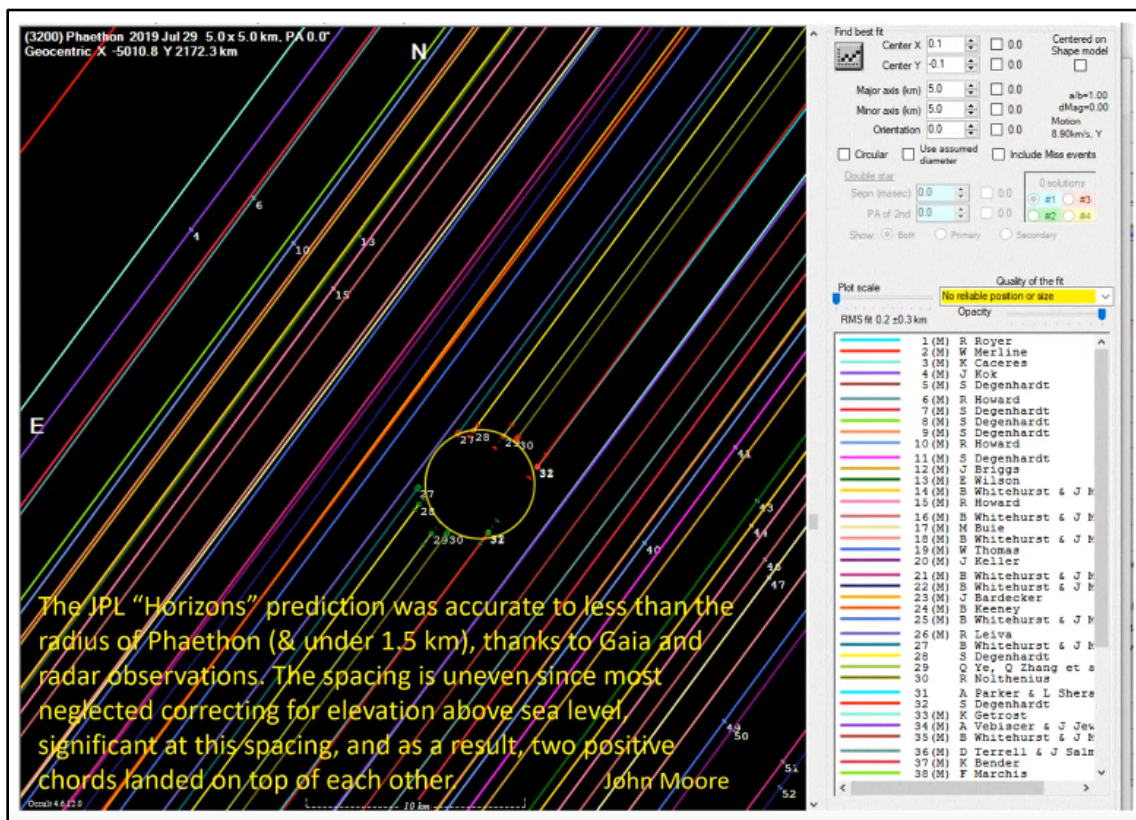


Figure 5. Occultation by (3200) Phaethon on 2019 Jul 29, all successful chords.

David then discussed how asteroid orbits are improved from asteroid occultations. This from a talk he gave at *JPL* while he was in Pasadena for the *NASA Small Bodies Assessment Group* on 2020 Jan 15. One such example occultation was the well observed (87) Sylvania event from 2019 Oct 29.

He showed a few occultation observations that match generally closely with the DAMIT shape models [9]. After a successfully observed occultation, a highly accurate astrometric position becomes available for both the star and asteroid. Along with the Gaia DR2 release (highest accurate star positions and proper motions to date) this has allowed further improvement on asteroid orbits for predicting a future event. David showed several observed asteroid occultations of how the accurate orbits and star positions have reduced the path errors significantly.

IOTA's Vice President **Dr. Roger Venable** talked about strange light curves he gets from the Watec 910HX camera system. Roger first showed the difference of *Limovie's* contour plots of unsaturated star peaks (pointed top) vs. saturated star peaks – (flat top). He warned about the *AVerMedia EZMaker* analog-to-digital converter which causes the star images to appear double. These faulty converters also give up and down light curve plots which on first glance appear to be noise. Not only does this converter cause the up and down effect, it degrades the star image aspect ratio to change from circular to rectangular in shape. Roger learned that the more saturation, the less of the up and down effect in the light curve (Figure 6).

Tony George commented that with his Watec 910HX camera, he has never seen this up/down effect in the light curves, which includes hundreds of observations he has analyzed over the years. He suspected the capture device and/or cables could be the cause of the sinusoidal effect in the light curves and not caused by the Watec 910HX camera. There was a disagreement on the origin of this effect as several other participants offered theories on what might be the source of this very strange anomaly.

**Oliver Klös** (on behalf of Konrad Guhl, IOTA/ES President) talked about IOTA/ES occultation activities. IOTA/ES is a very active IOTA organization, observing over a hundred occultations per year, publishing papers in *JOA* and heavily involved in numerous activities. In 2019 they had 180 positive reports, in 2020 they already have 134 positive reports. He highlighted the (2) Pallas 2020 June 22 event which had 34 positive chords. The (87) Sylvania event on 2019 Oct 29 was highly successful which included observations of Sylvania's 2 moons. Oliver mentioned if you have any type of occultation report or technique, please submit it to the *JOA* which is published by IOTA/ES.

The *European Symposium on Occultation projects* (ESOP) occurred this year on 2020 Aug 29/30. The meeting will be online only due to the Covid-19 situation. ESOP is a highly attended meeting, typically 70-80 people go [10]. IOTA/ES recently made a collective purchase of 31 QHY174M-GPS cameras. A workshop was held on 2020 Feb 29 on how to use the camera with all of its features and calibration settings.

The Meeting adjourned at 18:15 UT.

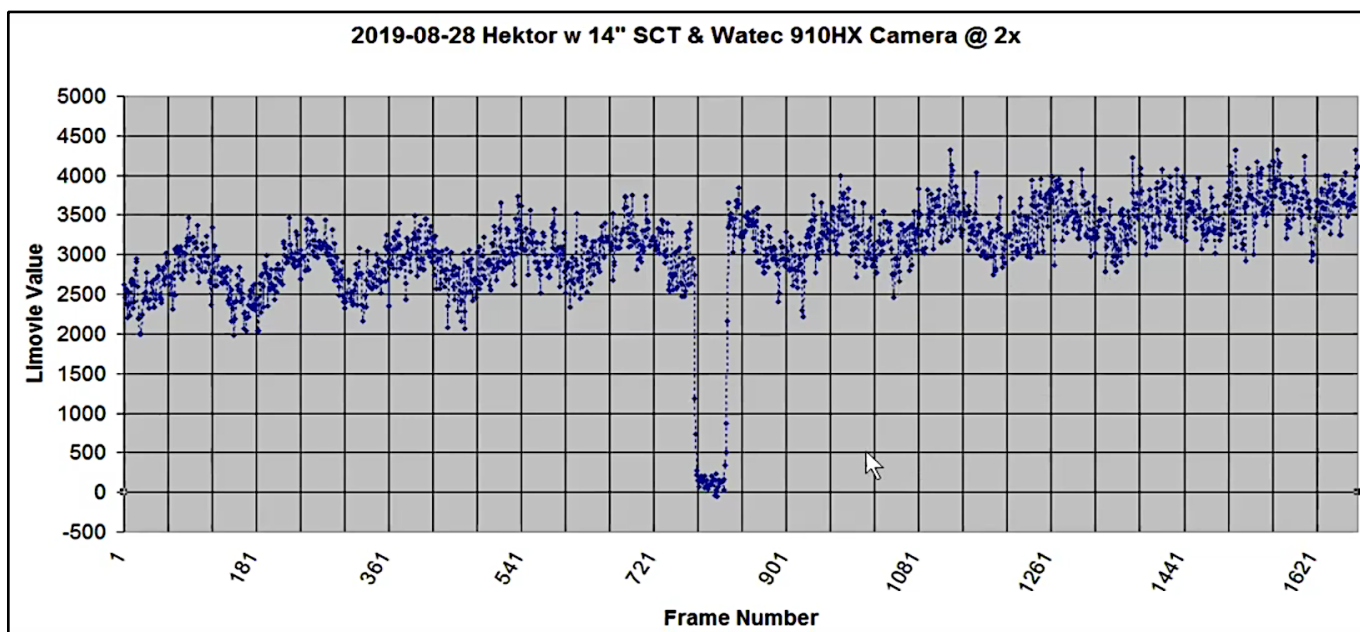


Figure 6. Up and down effect in the light curve of a recording of an occultation by (624) Hektor.

## References

- [1] IOTA's 2020 Meeting Schedule and Agenda  
<http://occultations.org/community/meetingsconferences/na/2020-iota-annual-meeting/>
- [2] IOTA's YouTube link and uploaded presentations  
[https://www.youtube.com/playlist?list=PLY2hxQmBE-LEB9AI-5NESPkPU6Lxkqf\\_G](https://www.youtube.com/playlist?list=PLY2hxQmBE-LEB9AI-5NESPkPU6Lxkqf_G)
- [3] MADAMO Award  
<https://pauldmaley.com/merline/#:~:text=The%20MADAMO%20award%20is%20to,monetary%20prize%20of%20US%244%2C000.>
- [4] IOTA's Award page  
<http://www.asteroidoccultations.com/observations/Awards/IOTA%20Awards.htm>
- [5] IOTA India Section  
<http://iota-india.in/>
- [6] Dunham, D. 2020 World Map for Grazes  
<http://iota.jhuapl.edu/GRAZEMAP.HTM>
- [7] Glover, R. *SharpCap* Forum on QYH Cameras  
<https://forums.sharpcap.co.uk/viewforum.php?f=28>
- [8] Weber, C. IOTA/ES Berlin Workshop Notes on the QHY174M-GPS  
[https://www.iota-es.de/qhy174gps\\_workshop.html](https://www.iota-es.de/qhy174gps_workshop.html)
- [9] DAMIT - Database of Asteroid Models from Inversion Techniques  
<https://astro.troja.mff.cuni.cz/projects/damit/>
- [10] Web Video Conference ESOP XXXIX  
<https://esop39.iota-es.de/>

## Breaking News

### New Version of Gaia Catalogue in *Occult* with Gaia EDR3 Coming Soon

2020 Dec 06

The Gaia Early Data Release (EDR3) was presented by ESA on 2020 Dec 03. Its content is essentially the same as in DR2, but with greater precision. The number of stars with astrometric solutions of 5 or 6 parameters has increased by more than 135,000,000 sources compared to DR2 [1].

Dave Herald updates now his Gaia catalogue for his *Occult* software with this new data. This work includes to generate a subset of EDR3 with the fields needed for occultation work.

He will be using the following EDR3 fields for the subset:

SOURCE\_ID, REF\_EPOCH, RA, RA\_ERROR, DEC, DEC\_ERROR, PARALLAX, PARALLAX\_ERROR, PMRA, PMRA\_ERROR, PMDEC, PMDEC\_ERROR, DR2\_RADIAL\_VELOCITY, DR2\_RADIAL\_VELOCITY\_ERROR, RUWE, DUPLICATED\_SOURCE, PHOT\_G\_MEAN\_MAG, PHOT\_BP\_MEAN\_MAG, PHOT\_RP\_MEAN\_MAG [2]

Having downloaded the required data (8.1 Gbytes), the next steps will be to put all data into binary format, to incorporate Hipparcos stars that are not in EDR3 (to ensure full coverage at the bright end) and to match the stars to HIP, Tycho-2 and UCAC4 catalogues to incorporate the star identifier in those catalogues, so that predictions and reductions use a convenient star identifier as has been used by the occultation observer community. Herald plans will be extending the coverage from all stars where the Gmag or Rmag was brighter than 14.0, to all stars where the Gmag is brighter than 15.0. [Gmag is essentially a Visual magnitude). As for DR2, Herald will provide the catalogue in the full version, which is expected to be about 40% larger than the current Gaia14\_DR2 file (due to both about 28% more stars, and more data items for each star). Herald will also provide the catalogue in at least one magnitude-limited version, so that a smaller version is available.

About the release date of his new version of the Gaia catalogue Herald wrote on the occultation mailing lists on 2020 Dec 4:

*I want to make sure I download all the fields we need for both predictions and reductions – and ensuring we have what we want is more important than speed [it will be a different story with the full DR3 – while the star data will remain unchanged, it will have orbital elements for >100,000 asteroids, which we will want to use as soon as possible]. Release in early 2021 is planned.*

His current hope is to be able to release the catalogue before the New Year. The new catalogue will have extra fields than the present catalogues, which will require significant changes within *Occult* in order for the catalogue to be used. These changes are likely to be the slowest part of the process. Watch out for more announcements on the mailing lists in the upcoming weeks!  
(OK)

[1] <https://www.cosmos.esa.int/web/gaia/earlyedr3>

[2] [https://gea.esac.esa.int/archive/documentation/GEDR3/Gaia\\_archive/chap\\_datamodel/](https://gea.esac.esa.int/archive/documentation/GEDR3/Gaia_archive/chap_datamodel/)



# Journal for Occultation Astronomy

## IOTA's Mission

The International Occultation Timing Association, Inc was established to encourage and facilitate the observation of occultations and eclipses. It provides predictions for grazing occultations of stars by the Moon and predictions for occultations of stars by asteroids and planets, information on observing equipment and techniques, and reports to the members of observations made.

The Journal for Occultation Astronomy (JOA) is published on behalf of IOTA, IOTA/ES and RASNZ and for the worldwide occultation astronomy community.

IOTA President: Steve Preston . . . . . [stevepr@acm.org](mailto:stevepr@acm.org)  
IOTA Executive Vice-President: Roger Venable . . . . . [rjvmd@hughes.net](mailto:rjvmd@hughes.net)  
IOTA Executive Secretary: Richard Nugent . . . . . [RNugent@wt.net](mailto:RNugent@wt.net)  
IOTA Secretary & Treasurer: Joan Dunham . . . . . [iotatreas@yahoo.com](mailto:iotatreas@yahoo.com)  
IOTA Vice President f. Grazing Occultation Services: Dr. Mitsuru Soma . . . . . [Mitsuru.Soma@gmail.com](mailto:Mitsuru.Soma@gmail.com)  
IOTA Vice President f. Lunar Occultation Services: Walt Robinson . . . . . [webmaster@lunar-occultations.com](mailto:webmaster@lunar-occultations.com)  
IOTA Vice President f. Planetary Occultation: John Moore . . . . . [reports@asteroidoccultation.com](mailto:reports@asteroidoccultation.com)  
IOTA/ES President: Konrad Guhl . . . . . [president@iota-es.de](mailto:president@iota-es.de)  
IOTA/ES Research & Development: Dr. Wolfgang Beisker . . . . . [wbeisker@iota-es.de](mailto:wbeisker@iota-es.de)  
IOTA/ES Treasurer: Andreas Tegtmeier . . . . . [treasurer@iota-es.de](mailto:treasurer@iota-es.de)  
IOTA/ES Public Relations: Oliver Klös . . . . . [PR@iota-es.de](mailto:PR@iota-es.de)  
IOTA/ES Secretary: Nikolai Wünsche . . . . . [secretary@iota-es.de](mailto:secretary@iota-es.de)  
RASNZ Occultation Section Director: Steve Kerr . . . . . [Director@occultations.org.nz](mailto:Director@occultations.org.nz)  
RASNZ President: John Drummond . . . . . [president@rasnz.org.nz](mailto:president@rasnz.org.nz)  
RASNZ Vice President: Nicholas Rattenbury . . . . . [nicholas.rattenbury@gmail.com](mailto:nicholas.rattenbury@gmail.com)  
RASNZ Secretary: Nichola Van der Aa . . . . . [secretary@rasnz.org.nz](mailto:secretary@rasnz.org.nz)  
RASNZ Treasurer: Simon Lowther . . . . . [treasurer@rasnz.org.nz](mailto:treasurer@rasnz.org.nz)

## Worldwide Partners

Club Eclipse (France) . . . . . [www.astrosurf.com/club\\_eclipse](http://www.astrosurf.com/club_eclipse)  
IOTA-India . . . . . <http://iota-india.in>  
IOTA/ME (Middle East) . . . . . [www.iota-me.com](http://www.iota-me.com)  
President: Atila Poro . . . . . [iotamiddleeast@yahoo.com](mailto:iotamiddleeast@yahoo.com)  
LIADA (Latin America) . . . . . [www.ocultacionesliada.wordpress.com](http://www.ocultacionesliada.wordpress.com)  
SOTAS (Stellar Occultation Timing Association Switzerland) . . . . . [www.occultations.ch](http://www.occultations.ch)

## Imprint

Publisher: IOTA/ES, Am Brombeerhag 13, D-30459 Hannover, Germany E-mail: [joa@iota-es.de](mailto:joa@iota-es.de)  
Responsible in Terms of the German Press Law (V.i.S.d.P.): Konrad Guhl  
Editorial Board: Wolfgang Beisker, Oliver Klös, Mike Kretlow, Alexander Pratt  
Additional Reviewers: Richard Miles, Christian Weber  
Layout Artist: Oliver Klös Original Layout by Michael Busse (†)  
Webmaster: Wolfgang Beisker, [wbeisker@iota-es.de](mailto:wbeisker@iota-es.de)  
Membership Fee IOTA/ES: 20,- Euro a year  
Publication Dates: 4 times a year

Submission Deadline for JOA 2021-2: February 15

## IOTA on the World Wide Web



IOTA maintains the following web sites for your information and rapid notification of events:

[www.occultations.org](http://www.occultations.org)  
[www.iota-es.de](http://www.iota-es.de)  
[www.occultations.org.nz](http://www.occultations.org.nz)

These sites contain information about the organization known as IOTA and provide information about joining.

The main page of [occultations.org](http://occultations.org) provides links to IOTA's major technical sites, as well as to the major IOTA sections, including those in Europe, Middle East, Australia/New Zealand, and South America.

The technical sites hold definitions and information about all issues of occultation methods. It contains also results for all different phenomena. Occultations by the Moon, by planets, asteroids and TNOs are presented. Solar eclipses as a special kind of occultation can be found there as well results of other timely phenomena such as mutual events of satellites and lunar meteor impact flashes.

IOTA and IOTA/ES have an on-line archive of all issues of Occultation Newsletter, IOTA'S predecessor to JOA.

## Journal for Occultation Astronomy

(ISSN 0737-6766) is published quarterly in the USA by the International Occultation Timing Association, Inc. (IOTA)  
PO Box 423, Greenbelt, MD 20768

IOTA is a tax-exempt organization under sections 501(c)(3) and 509(a)(2) of the Internal Revenue Code USA, and is incorporated in the state of Texas. Printed Circulation: 200

## Regulations

The Journal of Occultation Astronomy (JOA) is not covenanted to print articles it did not ask for.

The author is responsible for the contents of his article & pictures.

If necessary for any reason JOA can shorten an article but without changing its meaning or scientific contents.

JOA will always try to produce an article as soon as possible based to date & time of other articles it received – but actual announcements have the priority!

Articles can be reprinted in other Journals only if JOA has been asked for permission.